PROTEIN-PROTEIN INTERACTIONS IN THE CYTOCHROME P450 SYSTEM

Erin V. Shea

April 16, 2012

"This thesis has been read and approved by _____. Date: ___/___/___"

(Dr. Paul F. Hollenberg)

TABLE OF CONTENTS

List of Abbreviations

Cytochrome P450 ..... CYP or P450
Cytochrome P450 Reductase ..... CPR
Human Liver Micromsomes ..... HLM
Wild-Type ..... WT
Carbon Monoxide ..... CO
Electrospray Ionization Liquid Chromatography Mass Spectrometry ..... ESI-LC-MS
Flavin Mononucleotide ..... FMN
Millivolt ..... mV
Flavin Adenine Dinucleotide ..... FAD
Nicotinamide Adenine Dinucleotide Phosphate ..... NADPH
Dilauroylphosphatidylcholine ..... DLPC
Formaldehyde ..... HCHO
tert-Butyl Hydroperoxide ..... tBHP
Trifluoroacetic Acid ..... TFA
Trichloroacetic Acid ..... TCA
Benzphetamine ..... BNZ
para-Nitrophenol ..... p-NP
4-nitrocatechol 4-NC
Protein Data Bank ..... PDB
Endoplasmic Reticulum ..... ER

Abstract:

Cytochrome P450s (CYPs or P450s) requires an interaction with their physiological redox partner, cytochrome P450 reductase (CPR) for efficient catalysis. However *in vivo* CPR is in limited supply, existing in a 1:10 to 1:25 ratio to P450. Additionally, studies in both microsomal and reconstituted systems have shown that the presence of one P450 isoform can influence the catalytic activity of a different isoform. In our study, it was examined whether the presence of CYP2E1 would influence CYP2B4's catalytic properties. The data demonstrate that CYP2E1 acts a potent inhibitor of CYP2B4-mediated *N*-demethylation of benzphetamine (BNZ), with a K_i of 0.05 μM. CYP2B4 was found to be resistant to inhibition by CYP2E1 when an artificial oxidant, tert-butyl hydroperoxide, was used. Alternatively, CYP2B4 was unable to inhibit CYP2E1-mediated p-nitrophenol hydroxylation. While determining the apparent K_M of CYP2B4 for CPR in the presence of increasing concentrations of CYP2E1, a dual competitive and non-competitive nature of CYP2E1 inhibition was exposed. At low concentrations of CYP2E1, CYP2B4's K_M for CPR increased by 13-fold with virtually no change in k_{cat}. While at high concentrations of CYP2E1, CYP2B4's K_M decreased to levels comparable to those observed in the absence of CYP2E1, though the k_{cat} also decreased by 10-fold. Moreover, CYP2E1 increased the K_M of CYP2B4 for BNZ by 8-fold, however the K_M was only partly decreased to that observed in the absence of 2E1 with the use of saturating concentrations of CPR. CYP2B4 and CYP2E1's individual K_M for CPR are nearly equal. Yet, the K_M values of CYP2E1 for CPR in the presence of CYP2B4 deceases significantly. Therefore, these results suggest that the presence of CYP2B4 enhances CYP2E1's affinity for CPR, which may allow CYP2E1 to out-compete CYP2B4 for CPR.

Introduction:

1. A Brief History:

In 1958, the first report of cytochrome P450 (CYP or P450) was published by Klingenberg, who examined the absorption properties of P450s (*1*). He noted that of the heme containing proteins of the rat microsomes designated as cytochromes b_5, some had a characteristic absorbance at 450 nm upon binding of carbon monoxide (CO) and reduction of the heme. Further research by Omura and Sato established the name of this heme protein as cytochrome P450. They were able to separate what is now known as cytochrome P450 from cytochrome b_5 (*2*). Additionally, it was found that P420 is the denatured form of P450. From the initial identification of P450, their findings gave birth to an area of major interest in the field of drug metabolism, toxicity, and steroid biosynthesis to name a few.

Early investigators of cytochrome P450 examined the metabolic function of P450s. Specifically, they studied the metabolism of carcinogens, drugs, pesticides, vitamins, and steroids (*3, 4, 5, 6, 7*). Cytochrome P450 was found to catalyze monooxygenase reactions (*8*). The mechanism of metabolism and the elucidation of the P450 catalytic cycle have continued to be areas of great interest study. The various substrates are metabolized by the microsomal P450 system, which is made up of three components: cytochrome P450, cytochrome P450 reductase, and phospholipid (*9, 10*). By the late 1970s, researchers were able to purify microsomal P450s for further analysis of cytochrome P450, specifically functional analysis (*11, 12*).

As research continued, experimental evidence suggested that multiple isoforms of cytochrome P450 existed (*13,14)*. In the 1970s, with the development of new technology such as recombinant DNA and heterologous protein expressions, the hypothesis of multiple isoforms of P450s was confirmed (*15*). The increasing number of P450s identified created a need for a naming system and in 1987 Nebert and co-workers developed one based on sequence identity (*16*). The multiple isoforms of P450s have significantly different amino acid sequences. These isoforms follow a nomenclature based on the sequence of the proteins. The P450 name originates from the spectral absorbance at 450nm when a complex is formed between the reduced heme and CO. P450s within the same family share 40% sequence identity on the amino acid level; this gives the assignment of a number (1, 2, 3, etc.) to identity the protein (*26*). Similarly, P450s that are members of the same subfamily share 55% sequence identity, giving the designation of a letter (A, B, C, D, etc.) (*26*). The final number in P450 nomenclature marks (1, 2, 3, etc.) each individual cytochrome P450.

Another major milestone in P450 research was the first crystal structure of P450cam from *Pseudomonas putida*, which provided greater insight to the structure of the P450 superfamily (*17*). Since then, other isoforms of P450 crystal structures have been reported, such as CYP2D6 and 3A4 (*18, 19*). In recent years, cytochrome P450 research has been focused on hepatic P450s due to their involvement in drug metabolism and thus they are of great pharmaceutical concern in understanding bioavailability, drug-drug interactions and toxicity. Additionally, another area of on-going research is concerned with detailing the catalytic cycle along with P450 inhibitors, characterization of novel P450 isoforms, and continued efforts to crystalize different P450 isoforms (*20, 21, 22*).

2. Background on Cytochrome P450:

Cytochrome P450s are a large family of proteins that are found in most plants, animals, and in nearly every human cell type. Mammalian P450s are membrane-bound hemoproteins. P450 structures are highly conserved; they are dynamic with a rigid core. In general, P450 secondary structure consists of four to five beta sheets, eight to ten helices, and a central heme. The unique folds of P450s are specifically adapted for the function of oxygen activation by heme-thiolate chemistry, the binding of redox partners (cytochrome P450 reductase (CPR) or cytochrome b_5 (Cyt b_5)), and stereochemical selection of substrates (*23*). The different isoforms of P450 are more structurally conserved closer to the heme center, specifically conserving the structures involved in heme-thiolate oxygen chemistry. The high conservation can be seen in the helices I and L, which directly contact the heme. Along with I and L helices, the β-bulge contains the Cys, which coordinates with the heme iron. The Cys accepts a hydrogen bond from the peptide NH group, which helps to regulate the redox potential heme irons required for efficient P450 reactions. The greatest structural differences between the different isoforms can be seen in the areas controlling substrate specificity, such as the B' helix. The structure of CYP2B4, which is the topic of this study, can be seen with labeled helices and β sheets in Figure 1.

Figure 1: Cytochrome P450 2B4 with substrate bound. The sequence follows from the blue N-terminus to the red C-terminus, with the heme shown in red sticks. The major helices are labeled. The image was taken from Scott et. al., who generated the image from a crystal structure using PyMOL (*24*).

In the human liver, CYPs metabolize 60% of all exogenous compounds such as clinically used drugs. Additionally, P450s metabolize many endogenous substrates such as steroids, fatty acids, and lipid soluble vitamins. Furthermore, CYPs are known to transform some foreign chemicals into reactive toxins or mutagens. Cytochrome P450s are able to catalyze a wide variety of oxidative reactions, such as hydroxylation, epoxidation, *N*-, *S*-, and *O*-dealkyation, sulphoxidation, epoxidation, deamination, desulphuration, dehalogenation, nitrogen oxidation,

and peroxidation along with other oxidative reactions (*25*). The cytochrome P450 systems catalyze the following reaction scheme:

$$RH + O_2 + NAD(P)H + H^+ \rightarrow ROH + NAD(P)^+ + H_2O$$

The P450 superfamily is able to metabolize a diverse range of substrates in almost all types of organisms. The human liver is the primary site of drug metabolism by human P450s, thus these proteins are a topic of major medical research.

The combination of multiple isoforms along with the highly dynamic conformational nature of P450s plays a role in the ability of human liver's P450s to metabolize approximately 70% of all drugs, along with many steroids, fatty acids, and xenobiotics (*27, 28*). The metabolic fate of a drug is determined not only by the interactions of that specific drug with the P450(s) that metabolizes the drug, but also on the potential of co-administered drugs to modulate the metabolic capability of the drug metabolizing P450. For example, the co-administered drug may potentially induce the expression level of a P450 or the drug may directly inhibit the activity of the P450. With the induced expression of a P450, the metabolism of a drug may be dramatically increased, thus lowering the concentration of the drug and preventing any therapeutic effects. Additionally, elevated levels of an individual P450 may alter the physiological levels of potentially essential compounds such as signaling molecules or hormones. These changes in the concentration of P450 substrates can cause detrimental effects, such as drug-drug interactions. Furthermore, the inhibition of a P450 may prevent the metabolism of a compound and thus cause the accumulation of a drug or compound to harmful levels in the body. Due to these potentially adverse reactions, it is critical to have a thorough understanding of the P450 function and structure to predict and avoid potentially unfavorable drug-drug interactions. Additionally, it is

important to have a comprehensive understanding of P450 mechanism and structure to avoid potentially adverse reactions. Thus, it is critical to understand how co-administered drugs may alter one another's metabolism to prevent drug-drug interactions through the P450 metabolism system.

3. The Catalytic Cycle

For P450s to perform oxidative reactions, they depend on their interactions with their physiological redox partner, cytochrome P450 reductase (CPR). The P450 catalytic cycle reveals the critical role that CPR plays in P450 mediated metabolism. Research continues to elucidate new facets of the catalytic cycle. The overall catalytic cycle can be seen in Figure 2 (*33*). In the resting state, the heme iron is in the ferric state (Fe^{3+}) with an absorbance at 420 nm. The resting state of P450 is labeled as A in Figure 2. The catalytic cycle is initiated with the binding of the substrate, which displaces a water molecule as the sixth ligand for the heme iron. The binding of the substrate induces the transition of the heme iron from a low spin state to a high spin state, with an increase absorbance at 390 nm and a decrease on the absorbance at 420 nm which is referred to as a "Type I" difference spectrum (*29*). Due to the slight change of the iron position relative to the plane of the porphyrin ring, this transition subsequently increases the P450's redox potential from approximately -330 mV to -110 mV (*29*). This transition is illustrated in the Figure 2 as the shift from A to B. The change in redox potential results in the high spin P450 having a higher redox potential than the Flavin Mononucleatide (FMN) domain of CPR. Thus an electron is transferred from CPR to the P450, causing the reduction of ferric P450 to ferrous (Fe^{2+}) P450, which is now thermodynamically favorable. The ferrous P450 in the is marked as C in the Figure. In this new oxidation state, the heme iron allows for the capture

of molecular oxygen by the ferrous heme, forming a stable dioxygen adduct shown as D. In Figure 2, D to E illustrates the delivery of a second electron from either CPR or cytochrome b_5 that then allows for the activation of bound oxygen, which is often the rate limiting step (*29*). Next, a quick protonation step occurs forming the ferric hydroperoxy complex (Fe^{3+}-OOH), which is the first reactive species form and is known as "Compound 0" (*30*). "Compound 0" is labeled as E' in Figure 2. This leads to a second protonation concurrently with the heterolytic cleavage of the O – O bond to produce a water molecule along with the highly reactive ferryl-oxo species (Fe^{2+}=O^{*}), known as "Compound I". F in Figure 2 designates "Compound I". The reactivity of the cation radical allows for the insertion of an oxygen atom into the substrate (*30*). Finally, oxidation of the substrate by the oxyferryl intermediate results in product release and restores the ferric form of P450 (*31,32*).

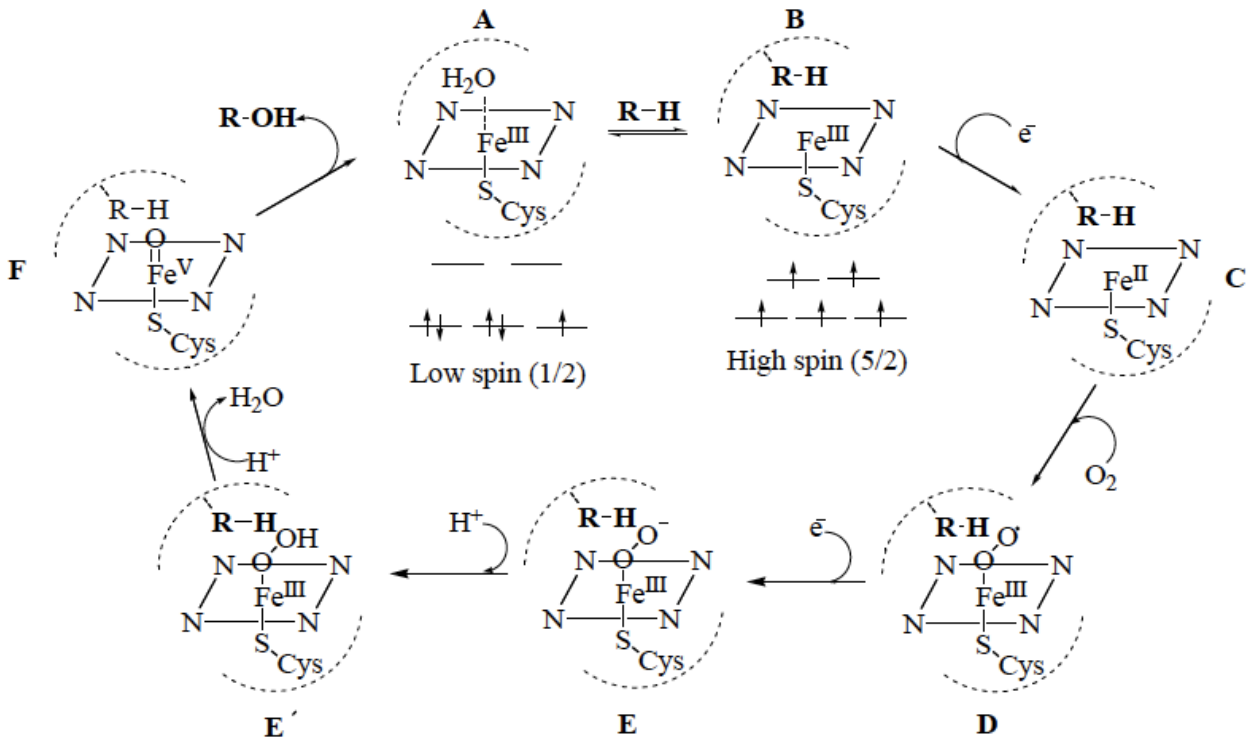

Figure 2: The Catalytic Cycle of an oxidative reaction by P450 taken from Bumpus (*33*).

The P450 catalytic cycle begins with A.

The majority of studies examining the catalytic properties of the P450 are performed in reconstituted systems and are typically conducted under saturating or near-saturating concentrations of CPR, where the CPR to P450 ratio is 1 or greater. However, under physiological conditions in the endoplasmic reticulum (ER), P450s are known to exist in vast excess over CPR. Many studies over the years have indicated that approximately 10 – 20 molecules of P450 are present in the ER for every single molecule of CPR (*34, 35, 36, 37*). Although there is a wealth of information about the mechanisms that direct the reduction of P450s by CPR, there is not much known about the spatial organization and distribution of P450, cytochromes b_5, and CPR within the membrane of the ER.

Over the past forty years, several models have been proposed to describe the distribution of P450s and their redox partners in the lipid membrane of the ER (*35, 36, 37, 38, 39*). One possible model that has been proposed is that the N-terminal hydrophobic tail of CPR firmly anchors the CPR in the membrane, while the CPR's catalytic domain protrudes from the membrane into the cytosolic region of the cell. In this model, it is envisioned that several P450s are clustered around a central CPR molecule and a portion of the microsomal P450s are loosely associated with the CPR and may be free-floating in the membrane (*34, 38*). The difference in the ratio between P450 to CPR (*34, 35, 36, 37*), along with the probable organization of these microsomal proteins in the membrane suggests that only a portion of the total microsomal P450s can be in a functional complex, at a given time. Thus, only a fraction of the total microsomal P450s are capable of drug metabolism at any given time. Furthermore, the un-complexed P450s that remain would fundamentally be rendered metabolically silent until they are able to form

functional interactions with CPR. Due to the limited number of CPR molecules relative to P450s, the outcome of P450-mediated drug metabolism may not just be a function of the particular P450 that metabolizes the drug. Thus, P450-mediated drug metabolism may also be a function of accessibility to CPR, which could be influenced by the presence and abundance of other P450s surrounding the CPR (*40*).

4. P450-P450 Interactions

In addition to potential drug-drug interactions in the cytochrome P450 system, there is also the possibility of protein-protein interactions that can lead to adverse reactions. There is increasing evidence that P450s in the liver that are involved in metabolism form complexes in the endoplasmic reticulum (*41*). The formation of a protein complex begins with collision between the proteins. As these collisions continue to occur, a complex begins to form through a transition state, moving through the energy landscape leading to lower energy state. The changes in energy follows a similar energy landscape as the fold of an individual protein (*42*). The formation of a protein complex is largely influenced by electrostatic interactions (*42*). Past studies by Schreiber showed the transitional state of the protein complex is stabilized by long-range electrostatic forces, which help to position the proteins before association (*43*).

Recent research has shown that both homomeric and heteromeric P450-P450 complexes form in the ER of the human liver, which can significantly alter cytochrome P450's function (*41*). Reed and Backes proposed that there are potentially three models of interaction between P450s, leading changes in each P450's activity (*41*).

The first model of interaction is just a simple competition between the two P450s for cytochrome P450 reductase, which is in limited supply. In this first model, the relative affinity of the P450s for CPR and the ability of the P450-CPR complex to oxidize the substrate will determine which P450 has greater metabolic activity. West and Lu examined interactions between CYP2B1 and CYP1A2 catalyzing the hydroxylation of 3,4-benzopyrene. They found that the interaction caused mutual inhibition by simple competition for CPR (*44*). Tan. et. al. similarly found that interactions between CYP2A6 and CYP2E1 are simply due to competition by the P450s for the CPR (*45*).

The second model of interaction is the potential formation of P450-P450 complex that affects cytochrome P450 binding to CPR. The physical complex formed between the two P450s leads to a change in the affinity of the P450s for CPR; the interaction may increase or decrease the affinity. Some experimental evidence of this was seen with the inhibition of CYP2B4 metabolism of 7-pentoxyresorufin in the presence of CYP1A2, while CYP1A2 metabolism of 7-ethoxyresorufin deethylation was shown to be stimulated by the presence of CYP2B4. Analysis of this data illustrated that the formation of a CYP1A2-CYP2B4 complex results in an enhancement of the CYP1A2 affinity for CPR (*34, 46, 47*).

A third model of interaction is the formation of a P450-P450 complex that affects the efficiency of substrate turnover. One study found evidence suggesting that 3A4 – mediated 6β-hydroxylation of testosterone was enhanced by up to four-fold in the presence of human, rat, and rabbit CYP1A2, though the degree of catalytic stimulation varied greatly depending on the species (*48*). Additionally, interactions between P450s have also been reported for other major

drug metabolizing enzymes, such as CYP2D6 and CYP2C9 (*49*). For this study, when CYP2D6 was co-incubated with CYP2C9, the results showed a 50% decrease in the V_{max} for the CYP2C9 mediated hydroxylation of flurbiprofen, while there was almost no observed change in the K_M. To determine the cause of inhibition at the pre-steady-state level, the K_s of CYP2C9 for flurbiprofen was measured in both the absence and presence of CYP2D6. The data showed that CYP2D6 increased the K_s of 2C9 for flurbiprofen by 20-fold. Thus, these results suggest that CYP2D6-mediated perturbation of CYP2C9's affinity for substrate is caused by conformational changes in the CYP2C9 active site architecture (*49*).

Additionally, the physiological relevance and implication of such interactions have been investigated. For example, the metabolism of methoxychlor by CYP2C19 has been shown to exhibit greater activity than CYP2C9 in a purified reconstituted system (*50*). When the role of CYP2C19 versus CYP2C9 for methoxychlor metabolism was assessed in HLM, conflicting results were found. Using monoclonal antibodies raised against CYP2C19, no change was observed in methoxychlor metabolism. However, antibodies raised against CYP2C9 were effective in inhibiting methoxychlor-O-demethylation (*51*). Finally, the metabolism of methoxychlor was examined in a binary reconstituted system that contained both CYP2C9 and CYP2C19. It was found that the demethylation of methoxychlor by CYP2C19 was significantly inhibited.

These results suggest that interactions between P450 isoforms can alter their catalytic rates and complicate *in vitro – in vivo* drug metabolism predictions. Some studies have shown that P450 isoforms in the ER also interact. Alston et al. showed that a complex between CYP1A1 and

CYP3A1/2 alters the metabolism of benzo[a]pyrene in the membrane *(52)*. Such studies illustrate that P450-P450 interactions may play a role in *in vivo* drug metabolism. In addition to the interactions between the P450 isoforms indicated here there is evidence to support interactions occurring between many more P450s. Some examples of isoform interactions include CYP2B4 and CYP1A2 (*45, 46, 47*), CYP1A2 and CYP2E1 *(53),* and CYP2C9 and CYP3A4 *(54)*

5. CYP2E1 and CYP2B6

The human liver contains many cytochrome P450s that play pharmaceutically important roles in the metabolism of drugs and toxins. Both the CYP2E1 and CYP2B6 isoforms are known to play significant roles in liver toxicity and drug metabolism, respectively.

Cytochrome P450 2E1 was first reported as an oxidant of ethanol over 40 years ago (*55*). It is estimated that CYP2E1 makes up 7% of the total P450 in the liver. This 7% of P450 in the liver is responsible for the metabolism of 10% of clinically used drugs. Several polymorphisms of CYP2E1 have been identified, although the significance of these polymorphism on *in vitro* and *in vivo* drug metabolism thus far has been shown to be negligible (*22*). Recently, the crystal structure of CYP2E1 was solved. This structure is the first experimental evidence of the isoform's uncommonly small active site (*56*). CYP2E1's active site is estimated to have a volume of 190 $Å^3$, rendering it the smallest known mammalian P450 active site thus far. CYP2E1 is known to bioactivate many low molecular weight compounds such as acetaminophen *(57),* N-ethyl nitrosamine (*58*) and carbon tetrachloride (*59*). It is also known that CYP2E1 is a highly uncoupled P450. CYP2E1 is known to be highly inducible. Induction of CYP2E1 protein

levels by alcohol (*60*) or fasting (*61*) likely contributes to an increase in the generation of reactive oxygen species (*62*). The increase in reactive oxygen species can lead to oxidative stress. CYP2E1s are of clinical interest due to their oxidation of particular drugs, oxidative stress, and activations of certain carcinogens.

Approximately 1-5% of the total P450 in the liver is comprised of CYP2B6, and this metabolizes approximately 5% of clinically used drugs (*22*). CYP2B6 plays an important role in the metabolism of a number of clinically important drugs, such as bupropion, cyclophosphamide, tamoxifen, efavirenz, and sertraline (*63, 64*). Additionally, CYP2B6 is known to metabolize nicotine. CYP2B6 has been found to be involved in the activation of some carcinogens. CYP2B6 has a highly polymorphic nature, which is of great importance in drug development because differences in amino acid composition are known to affect drug efficacy and toxicity. Nine single nucleotide polymorphisms have been identified, with 2B4K262R being the most common polymorphism. Unfortunately, the current heterologous expression system for recombinant human CYP2B6 in *E. coli.* has a very low yield. Thus, the more highly expressing rabbit CYP2B4 is used as a model system to understand metabolism by CYP2B6 (*65, 66*). CYP2B4 is known to share approximately 80% sequence similarity with CYP2B6, and the CYP2B4 structure was recently shown to be effectively identical to CYP2B6 (*67*).

Very little is known about how CYP2B4 and CYP2E1 interact with each other to modulate their catalytic activities, despite each having been studied extensively for their individual roles on metabolism and toxicity. Hence, the purpose of this study was to assess, in a purified reconstituted system, whether CYP2E1 and CYP2B4 could influence each other's metabolism

and then characterize the kinetic nature of such interactions. Finally, this study will propose a preliminary model that explains the physical basis for the kinetic results.

Materials and Methods:

Chemicals used during the project are all ACS grade and obtained from commercial vendors unless otherwise stated. The chemicals purchased from Sigma were benzphetamine, p-nitrophenol, NADPH, sodium dithionite, ascorbic acid and tert-butyl hydroperoxide. Trifluoroacetic acid was purchased from Pierce Chemicals. Dilauroylphosphatidylcholine (DLPC) was purchased from Doosan Serdary Research Laboratory (Toronto, Canada). Carbon monoxide gas (purity >99.5%) was purchased from Cryogenic Gases (Detroit, MI).

Construction of the CYP2E1 Y422D variant. A QuickChange site-directed mutagenesis kit was used to preform site-directed mutagenesis according to the manufacturer's protocol (Stratagene). The forward and reverse mutagenic primers for Y422D are GGAAAGTTCAAGGACAGTGACTATTTCAAGCC and GGCTTGAAATAGTCACTGTCCT TGAACTTTCC, respectively. The University of Michigan's DNA Sequencing Core completed DNA sequencing to confirm the site-specific mutation.

Overexpression and Purification of Enzymes. Dr. James Halpert generously gave us the plasmids for the N-terminal truncated and C-terminal His-tagged CYP2B4dH (referred to as CYP2B4) and human CYP2E1. Both the P450s and the CYP2E1 Y422D were over-expressed in *Escherichia* coli C41 (DE3) cells separately and purified using a Ni-NTA affinity column as described previously (*68, 69*). The concentrations of CYP2B4 and CYP2E1 were determined using an extinction coefficient of $\Delta\varepsilon_{450\text{-}490\ nm}$ of 91 mM cm^{-1} as described by Omura and Sato (*2*). Additionally, NADPH-dependent cytochrome P450 reductase (CPR) was expressed and purified from *Escherichia coli* also as described previously (*70*). The extinction coefficient of 21 mM cm^{-1} at 456nm was used to determine the concentration of CPR for the oxidized enzyme (*71*).

Determination of the Inhibition of CYP2B4 – Mediated N-demethylation of BNZ by CYP2E1 WT and the CYP2E1 Y422D variant. The extent to which varying concentrations of either CYP2E1 WT or CYP2E1 Y422D inhibited the rate of formaldehyde formation by CYP2B4 (0.25 μM) was assessed at 37^{o}C using a fixed concentration of CPR (0.5 μM) and BNZ (1.2 mM). CYP2B4 was reconstituted in triplicate with increasing concentrations of 0.25, 0.5, 0.75, 1.0, 1.25, 1.50 μM of CYP2E1 WT or CYP2E1 Y422D, CPR and 0.03 mg/ml DLPC on ice for 1 h. The reconstituted mixtures were then combined with 50 mM potassium phosphate buffer (pH 7.4) and benzphetamine. The samples where equilibrated at 37°C for 15 minutes. The reactions were initiated in the samples by adding 7.5 μL of 20 mM NADPH for a final reaction volume of 500 μL. The incubations proceeded for 5 minutes at 37°C before being quenched by the addition of 25 μL of 50% TFA. Next, the protein was precipitated by centrifugation at 13.2k rpm for 5 minutes. Finally, a 500 μL aliquot of the supernatant was assayed for formaldehyde using the Nash reaction (*72*)

Difference Spectra of the Carbon-Monoxy ferrous WT CYP2E1 and Y422D variant. CYP2E1 WT and the Y422D mutant (0.5 nml) were reconstituted with CPR (1 nmol) at 22°C for 30 min in 0.5 ml of suspension buffer (100 mM potassium phosphate, 20% glycerol and 0.1 mM EDTA, pH 7.4). 100 μM 4-methylpyrazole and 0.5 mM NADPH were added to the sample for the baseline, then the samples were bubbled with CO. The visible absorbance spectra were determined by scanning from 400 to 500 nm on a UV-2501PC spectrophotometer (Shimadzu Corporation, Kyoto, Japan) until a steady state was attained with no further changes. A trace

amount of sodium dithionite was added and additional scans were performed until no further change was detected.

Determination of the Apparent K_m and k_{cat} Values for CYP2B4 for CPR Using the N-demethylation of Benzphetamine in the Presence and Absence of CYP2E1. At 37°C, the rate of formaldehyde formation as a result of the N-demethylation of benzphetamine was measured at a constant P450 concentration with increasing concentration of CPR to determine the K_m and k_{cat} values of the CYP2B4 WT for CPR, as previously described (*73*). CYP2B4 WT (0.25 µM) was reconstituted in triplicate with varying concentrations of CPR (0.1, 0.2, 0.3, 0.6, 0.8, 1.2 and 1.4 µM) and 0.03 mg/ml DLPC on ice for 1 h. The reconstituted mixtures were added to 50 mM potassium phosphate buffer (pH 7.4) and 1.2 mM BNZ. The samples were allowed to equilibrate at 37° C for 15 minutes. Then the reactions were initiated by adding 7.5 µL of 20 mM NADPH for a final reaction volume of 500 µL. The reactions were incubated for 5 minutes at 37 ° C before being quenched by the addition of 25 µL of 50% TFA. The samples were centrifuged at 13.2k rpm for 5 minutes to precipitate the proteins. Then a 500 µL aliquot of the supernatant was assayed for formaldehyde using the Nash reaction. GraphPad Prism 5.0 from GraphPad Software (La Jolla, CA) was used to fit the data to the Michaelis – Menten equation to determine the kinetic parameters. To assess the effect of CYP2E1 on the K_m and k_{cat} of the CYP2B4 – CPR complex, the procedure outlined above was repeated in the presence of 0.125, 0.25, 0.75, 1.25, and 1.50 µM CYP2E1.

Graphical Analysis of Steady-State Activity Data. Using GraphPad Prism, a Lineweaver-Burk plot was obtained using the inverse of the reaction velocities obtained for the determination

of the K_m and k_{cat} values for CYP2B4 and CPR. These were plotted against the inverse of the concentrations of CPR used under varying concentrations of CYP2E1. The K_i was obtained for CYP2E1 as a competitive inhibitor of CYP2B4 – CPR complex by using two methods. First, a non-linear global fitting analysis of the data was done using GraphPad Prism. The second method involved plotting $K_{m\ obs}$ against varying concentrations of CYP2E1. The K_i was obtained from the *x*-intercept of a linear regression analysis of this plotted data (*74*).

Characterization of the tert-Butyl Hydroperoxide-supported Metabolism of Benzphetamine by CYP2B4 WT in the Presence of Increasing Concentrations of CYP2E1 WT. To establish the rates for the tert-butyl hydroperoxide-supported metabolism of benzphetamine, a final concentration of 0.25 μM CYP2B4 WT was incubated at 37°C for 15 minutes with 0.03 mg/ml DLPC, 50 mM potassium phosphate buffer (pH 7.4), and 1.2 mM benzphetamine. Then, 52.5 μL of 1 M tert-butyl hydroperoxide was added, resulting in a final volume of 500 μL. The reactions were allowed to proceed for 5 minutes, after which they were terminated by the addition of 20 μL of 50% TFA. Following termination, the samples were centrifuged at 13.2k rpm for 5 minutes and 500 μL aliquots of the supernatants were assayed for formaldehyde using the Nash Reaction. This procedure was then repeated in the presence of 0.25, 0.5, 0.75, 1.0, 1.25, 1.50 μM of CYP2E1 WT.

Determination of the K_m and k_{cat} Values for the Metabolism of Benzphetamine by CYP2B4 in the Absence and Presence of CYP2E1 WT. The K_m and k_{cat} values for BNZ metabolism by CYP2B4, in the absence and presence of CYP2E1, were determined at 37°C at constant P450 and CPR concentration with increasing concentrations of BNZ. The CYP2B4 WT protein (0.50

μM) was reconstituted in triplicate with equal concentration of CPR and 0.03 mg/ml DLPC with and without 2 μM of CYP2E1 WT on ice for 1 hour. Next, the reconstituted mixtures were added to 50mM potassium phosphate buffer (pH 7.4) with varying concentrations of benzphetamine, 0.05, 0.1, 0.2, 0.4, 0.6, and 0.8 μM. The samples were equilibrated at 37°C for 15 minutes. Then the reactions were initiated by adding 7.5 μL of 20 mM NADPH for a final reaction volume of 500 μL. The incubations proceeded for 5 minutes at 37°C and then were quenched by the addition of 25 μL of 50% TFA. The protein was then precipitated by centrifugation at 13.2k rpm for 5 minutes and 500 μL aliquots of the supernatant was assayed for formaldehyde formation using the Nash reaction. Next, it was tested whether the K_m could be decreased to the initial value in the absence of 2E1 by using saturating concentrations of CPR. This experiment was repeated in the presence of 2.5 μM CPR. Using GraphPad Prism 5.0, the data were fit to the Michaelis – Menten equation to determine the kinetic parameters.

Spectral Dissociation Constant (K_s) for the binding of BNZ to CYP2B4 in the Absence and Presence of CYP2E1. The previously mentioned measurement of type I spectral changes was used to spectrophotometrically monitor BNZ binding to ferric CYP2B4 (*75*). Equal volumes of P450 solutions containing 1 μM CYP2B4 in the presence or absence of 4 μM CYP2E1, 0.1 M potassium phosphate (pH 7.4) and 0.1 mg/ml DLPC were added to both the sample and the reference cuvettes. The baseline was recorded after thermal equilibration at 30°C for 5 minutes. CYP2B4 in the sample cuvette was titrated with aliquots of 20 mM BNZ, while equal volume of water was added to the reference cuvette. The difference spectra were recorded from 350-500 nm. The difference in absorbance between the wavelength maximum (386 nm) and the minimum (421 nm) were plotted as a function of varying BNZ concentration (5-1200 μM). The data was

then used to obtain the K_s by fitting to Equation 1.

$$\Delta A = \frac{\Delta A_{max} \times [BNZ]}{K_s + [BNZ]} \quad \textbf{Eq. 1}$$

Determination of the Apparent K_m and k_{cat} Values of CYP2E1 for CPR Using Hydroxylation of p-nitrophenol in the Absence and Presence of CYP2B4. At saturating concentrations of pNP, a fixed concentration of CYP2E1 and varying concentrations of CPR were used to determine the K_M and k_{cat} of CYP2E1 for CPR. Samples of 0.1 μM of CYP2E1 were reconstituted with varying concentrations of CPR (0.08, 0.12, 0.24, 0.72, 1.44, 2.00 μM) and 0.03 mg/ml DLPC in the presence and absence of 0.1 μM of CYP2B4 on ice for 1 hr. Next, the reconstituted mixtures were added to 50 mM of potassium phosphate buffer (pH 7.4), 0.3 mM pNP, and 2.0 mM ascorbic acid. The samples were allowed to equilibrate at 37°C for 15 minutes. Once equilibrated, the reactions were initiated by adding 20 μL of 20 mM NADPH for a final reaction volume of 1000 μL. The reactions proceeded for 20 minutes at 37°C and then they were quenched by 300 μL 20% TCA. After quenching the reactions, the samples were incubated on ice for 10 minutes and then centrifuged at 13.2k rpm for 5 minutes. The samples absorbance of the samples was then measured at 510 nm by transferring a 1000 μL aliquot to a cuvette containing 100 μL of 10M NaOH.

Results:

Effect of Increasing Concentrations of CYP2E1 on BNZ metabolism by CYP2B4. It has been previously established that CYP2B4 N-demethylates BNZ to form primarily norbenzphetamine and formaldehyde under the experimental conditions used in this assay. The product, formaldehyde is then reacted with the Nash reagent to form a conjugate species that absorbs maximally at 412 nm. Hence, for these studies it is necessary preclude the possibility that CYP2E1 metabolizes BNZ to form formaldehyde or any other product detectable by this assay. Previously established methods were used to determine CYP2E1 metabolism of BNZ. The results demonstrate the BNZ is primarily metabolized to nor-benzphetamine by CYP2B4 (data not shown). Additionally, the data showed that metabolism of BNZ by CYP2E1 is insignificant compared to CYP2B4, even at high concentrations of CYP2E1 (data not shown). The converse was also shown to be true for p-NP metabolism by CYP2E1. Thus these control experiments established that the N-demethylation of BNZ activity to form formaldehyde is specific for CYP2B4 activity, while the hydroxylation of p-NP to form 4-NC is specific for CYP2E1 activity.

Increasing concentrations of CYP2E1 were reconstituted with CYP2B4, CPR, and DLPC to determine the extent to which CYP2E1 could inhibit the catalytic activity of CYP2B4 toward its probe substrate BNZ. Increasing concentrations of CYP2E1 inhibit the activity of CYP2B4, up to approximately 80% loss of activity was observed in the presence of CYP2E1 compared to in the absence of CYP2E1, which can be seen in Figure 3. Additionally, the data show that inhibition can be fit to a rectangular hyperbolic function and follows saturation kinetics. The BNZ catalytic activity supported

by tBHP was characterized and compared to that supported by CPR. These studies were used to determine whether the decrease in activity is due to disruption of the interaction of CYP2B4 with CPR or due to direct interaction between CYP2B4 and CYP2E1 that decreases the catalytic activity of the 2B4. Hydroperoxides and other artificial oxygen donors are able to support the catalytic turnover of P450s in the absence of redox partners such as CPR. When the effect of increasing concentrations of 2E1 on BNZ mechanism by 2B4 was determined in the presence of tBHP, CYP2B4 was barely inhibited by CYP2E1. Thus the decrease in the CPR – supported BNZ activity suggests inhibition is not likely due directly to CYP2B4 – CYP2E1 interactions, but instead due to an effect on CPR – 2B4 interactions.

Additionally, the ability of CYP2B4 to modulate the metabolism of p-NP by CYP2E1 was examined. The results of these investigations are shown in Figure 3B. They demonstrate that CYP2B4 does not inhibit the catalytic activity of CYP2E1 and that the inhibition detected in the mixed reconstituted system is solely a property of CYP2E1 toward CYP2B4.

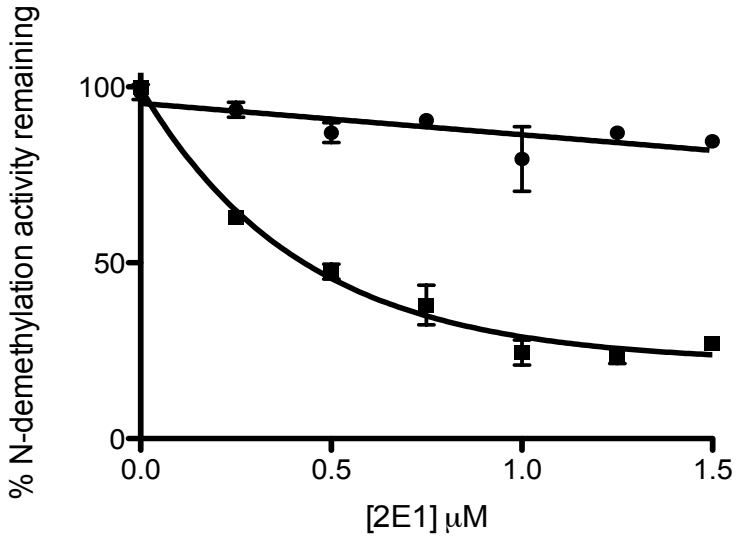

Figure 3A. CYP2B4 mediated N-demethylation of BNZ in the presence of increasing concentrations of CYP2E1. The rate of BNZ N-demethylation by CYP2B4 was assessed as described in Material and Methods. Formaldehyde formation was measured using either CPR/NADPH (■) or t-BHP (•), to support the activity to try to distinguish between the effects of direct CYP2E1 – CYP2B4 interactions on CYP2B4 activity versus competition for CPR. Saturating BNZ (1.2mM) was used to compensate for any possible perturbation in substrate binding affinity perpetrated by direct P450-P450 interactions.

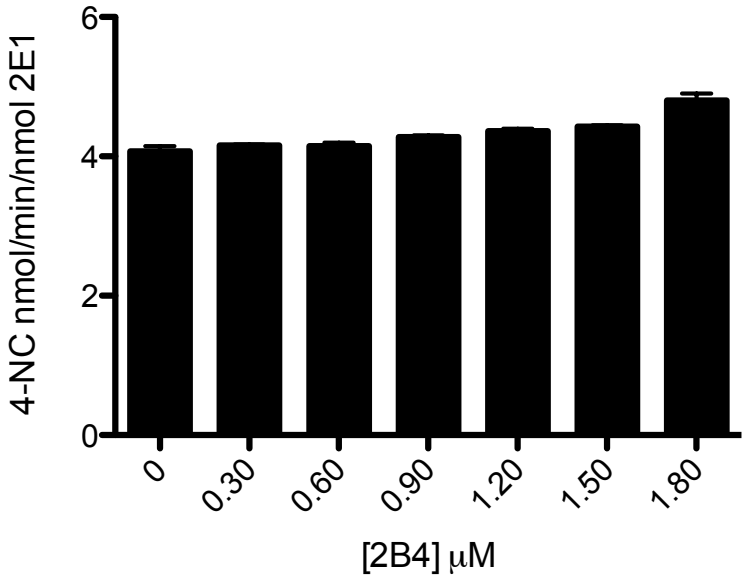

Figure 3B. CYP2E1 mediated p-NP hydroxylation in the presence of increasing concentrations of CYP2B4. The CYP2E1 – mediated hydroxylation of p-NP was assessed in the presence of increasing concentrations of CYP2B4 and saturating p-NP. The data points for BNZ and p-NP metabolism represent the mean of three triplicate experiments. The error bars represent the standard deviations.

Inhibition of CYP2B4 activity by the Y422D variant of CYP2E1. The conclusions described by Lin et. al. (*76*) led us to express and purify CYP2E1 Y422D to analyze whether the inhibitory event seen in Figure 3A was caused by the CYP2E1 – CPR interactions. The Y422 residue of CYP2E1 has previously been shown to be nitrated by peroxynitrite. This modification contributed to a loss in CPR – supported CYP2E1 activity when compared to the tBHP-supported activity. It is postulated that the highly negatively charged FMN domain of CPR interacts with the proximal side of CYP2E1 and therefore, we hypothesized that replacing Tyr with Asp by site-directed mutagenesis

would create a charge repulsive interaction between CYP2E1 Y422D and its residue counterpart in CPR. This charge repulsion would then perturb the apparent affinity of the two proteins for one another. Our lab's previous stopped-flow studies have shown that the extent of formation of the reduced CO – complex supported by NADPH is an indicator of the degree of P450 – CPR complex formation. This reflects the affinity of the P450 under investigation for CPR (*73*). The extent of Y422D reduction by CPR and NADPH compared to reduction of WT enzyme by CPR and NADPH can be established by measuring the absorbance of Y422D–CO complex at 450 nm and comparing this to the absorbance of WT-CO complex at 450 nm. The results shown in Figure 4A demonstrate that the interaction of CYP2E1 Y422D with CPR decreases by more than 50% compared to the WT. The inhibitory potential of the Y244D mutant was examined with CYP2B4. The results show that it inhibited the activity of CYP2B1 to a significantly lesser extent than CYP2E1 WT as can be seen in Figure 4B.

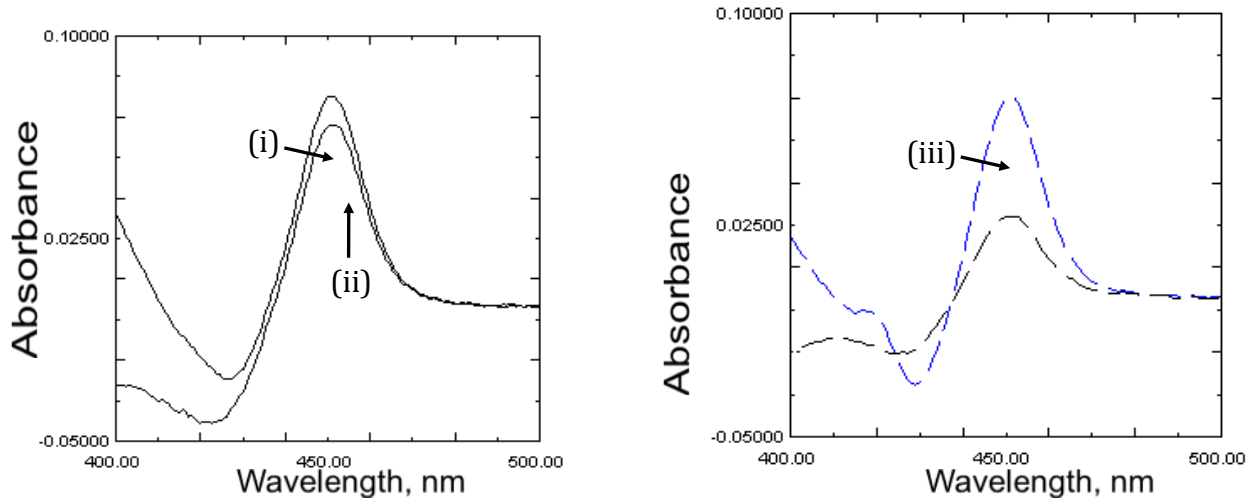

Figure 4A. Reduced CO spectra of WT CYP2E1 (left graph) and the CYP2E1 Y422D variant (right graph). In order to determine whether the mutation of Try 422 to Asp perturbed the binding of CPR to this variant, the CO absorbance difference spectrum was measured in the presence of CPR and NADPH following reconstitution, ensuring complete complex formation. Samples (i) and (iii) were chemically reduced with dithionite while samples (ii) and (iv) were reconstituted with CPR and reduced by addition of NADPH.

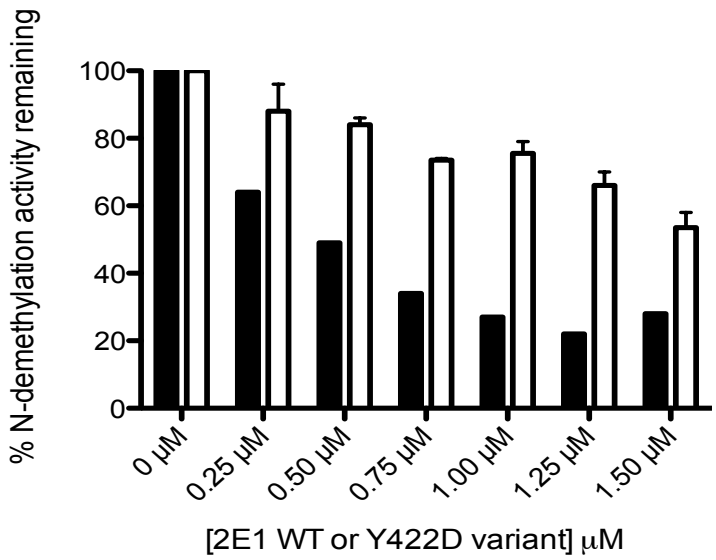

Figure 4B. The inhibition of CYP2B4 BNZ activity by CYP2E1 Y422D. To establish the role of CYP2E1 in the inhibition seen in Figure 3A, Y422D was evaluated with regard to its ability to inhibit CYP2B4 activity (open bars) and then compared to WT CYP2E1 (filled bars).

Determining the K_M and k_{cat} Values for the Interaction of CYP2B4 WT with CPR. The formation of a complex between CPR and CYP is an essential step in the transfer of electrons to the heme of the CYP that is required for substrate oxidation in the catalytic cycle. The rate of substrate oxidation has been proposed to be directly proportional to the concentration of CPR – CYP2B4 complex (*77, 78*). Therefore, measuring the rate of BNZ oxidation by a fixed concentration of CYP2B4 with the addition of increasing concentrations of CPR can be used to determine the K_M and k_{cat} of 2B4 for CPR across a range of CYP2E1 concentrations. Comparison of these kinetic parameters determined in the presence of increasing concentrations of CYP2E1 can be used to examine the kinetic nature of the inhibitory interaction, as illustrated in Figure 3A. Competition between

CYP2E1 and CYP2B4 should disrupt formation of the CYP2B4 – CPR catalytic formation and thereby increase the concentration of un-complexed CYP2B4. The un-complexed CYP2B4 would be unable to oxidize substrate, thus leaving it metabolically silent. Figure 5 shows that the rate of BNZ oxidation as a function of varying CPR concentrations follows a rectangular hyperbolic relationship, which can then be fit to the Michaelis – Menten equation, and that the addition of increasing concentrations of 2E1 does not alter that relationship but, does inhibit BNZ in a concentration-dependent manner. CYP2E1 concentrations between 0.125 - 0.75 μM increased the K_M of CYP2B4 for CPR by 14 fold, while the k_{cat} remains practically the unchanged. This is demonstrated in Figure 5 and Table 1.

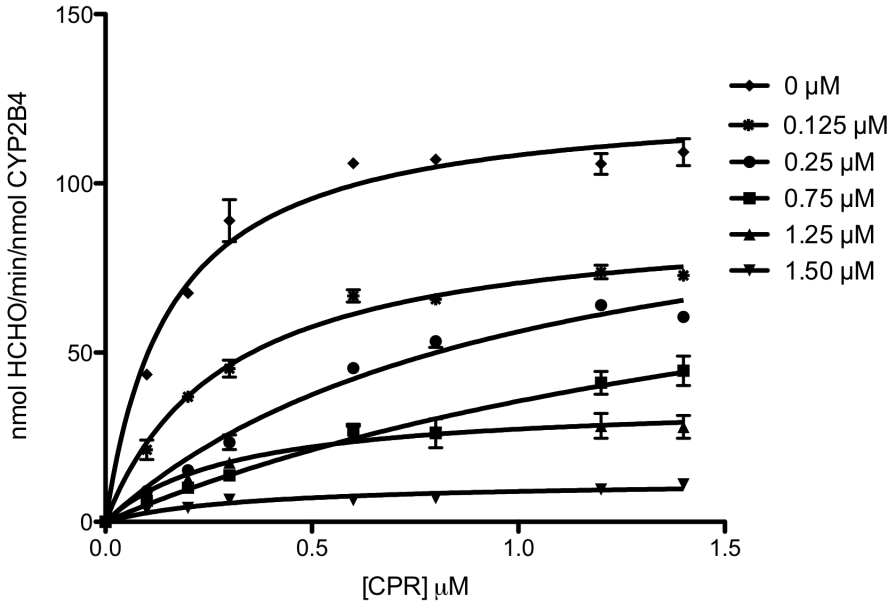

Figure 5. Determination the apparent K_M and k_{cat} values of CYP2B4 for CPR in the presence of increasing concentrations of CYP2E1 WT. The formation of formaldehyde was measured at a constant concentration of CYP2B4 (0.2 μM) with increasing concentrations of CPR as indicated in the presence of varying concentrations

of CYP2E1 WT. These measurements were done as described in Materials and Methods. The error bars on the graph are the standard deviations from the three measurements.

Table 1

[2E1] μM	$K_{M\ CYP2B4\text{-}CPR}$ (μM)	$k_{cat\ CYP2B4\text{-}CPR}$ (min^{-1})
0.00	0.16 ± 0.030	130.0 ± 3.9
0.125	0.29 ± 0.028	91.1 ± 2.8
0.25	0.99 ± 0.18	110. ± 11.
0.75	2.1 ± 0.73	110. ± 26.
1.25	0.31 ± 0.078	36. ± 3.0
1.50	0.36 ± 0.11	12. ± 1.3

Table 1. Determination of K_m and k_{cat} values for the interactions of CYP2B4 and CPR in the presences of increasing concentrations of CYP2E1 WT. The K_M and k_{cat} values were determined from the data in Figure 5 as described in Materials and Methods.

Concentrations of CYP2E1 above 0.75 μM exhibited an unusual kinetic behavior observed with the k_{cat} decreasing by 10-fold, while the K_M value decreased to 0.36 μM in the presence of 1.50 μM CYP2E1.

Linear Regression Analysis of the Steady-State Activity Data. Plotting the inverse of the BNZ activity against the inverse of CPR concentrations as a function of varying CYP2E1 concentrations showed that the steady – state activity data could be divided into two sets based on whether the linear regression analysis intersected at a common value on the *y*-axis but diverged on the *x*-axis or whether they diverged on the *y*-axis and intersected on the *x*-axis. Figure 6A shows that for the lower concentrations of 2E1 (0.0 to 0.75 μM), CYP2E1 behaves as a competitive inhibitor since the K_M increases

significantly, while the k_{cat} remains relatively unchanged. Figure 6B demonstrates the non-competitive inhibition by CYP2E1 with a K_M value for 1.25 and 1.50 μM CYP2E1 that is relatively similar to the K_M observed in the absence of CYP2E1, while the k_{cat} decreases significantly. Thus, CYP2E1 appears to inhibit formation of the CYP2B4 – CPR complex by acting as a competitive inhibitor at low concentrations and at high concentrations it acts as a noncompetitive inhibitor of the CYP2B4 – CPR complex formation.

Figure 6A.

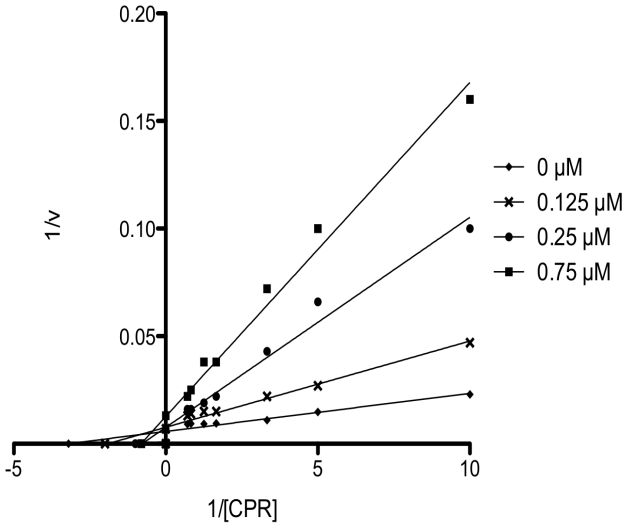

Figure 6B

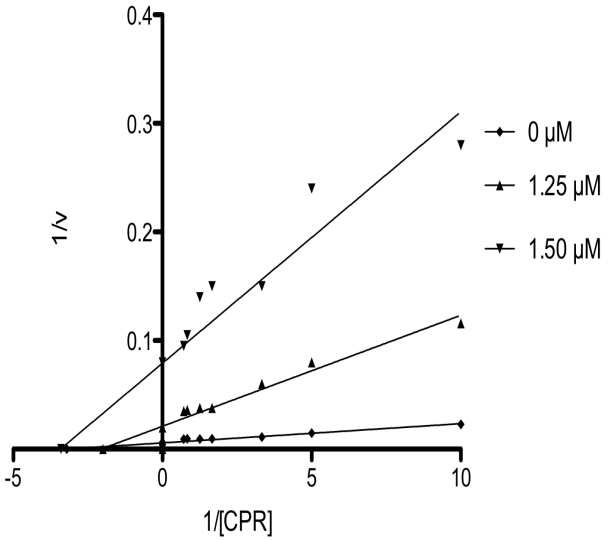

Figure 6. Lineweaver – Burk Plot of the Steady-State Activity Data Shown in Figure 5. From plotting the inverse rate of formaldehyde formation against the inverse of CPR concentration as a function of varying CYP2E1 concentrations, we observed that this data could be divided into sets based on whether the linear regression intersection occurs at a common intercept. With concentrations of CYP2E1 WT between 0 – 0.75 µM, the CYP 2E1 displayed competitive inhibition kinetics, seen in Figure 6A. While at higher

concentrations of CYP2E1, CYP2E1 behaved as a noncompetitive, as seen in Figure 6B.

In order to estimate the K_i for CYP2E1 as a competitive inhibitor of CYP2B4 – CPR complex formation the $K_{M\ obs}$ was plotted as a function of the CYP2E1 concentration. The data were fit to a straight line that intersected with the *x*-axis at an absolute value of 0.05 μM as is shown in Figure 7. Consequently, CYP2E1 is an effective inhibitor of CPR binding to CYP2B4 with a nanomolar affinity.

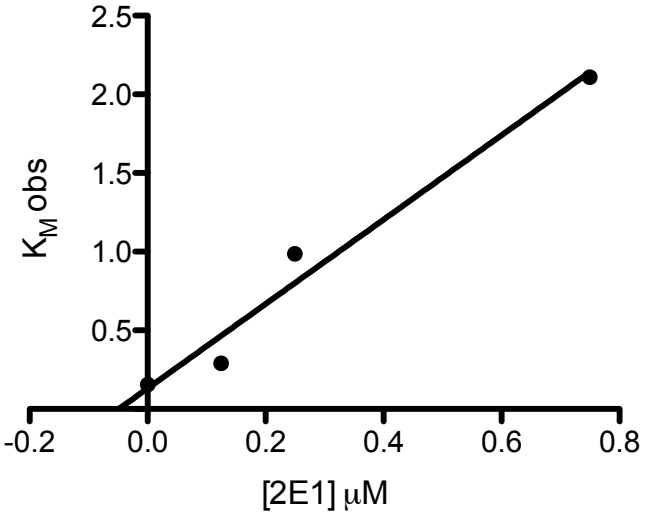

Figure 7. Plot of $K_{M\ obs}$ versus CYP2E1 concentration. The $K_{M\ app}$ values were obtained from study of the activity data in Figure 5. The linear regression analysis for CYP2E1 concentrations ranging from 0 to 0.75 μM is shown as the solid line on the graph. The K_i is determined from the absolute value of the *x*-intercept of the line.

Steady-state activity of CYP2B4 for BNZ metabolism in the presence and absence of CYP2E1. It has been previously suggested that there is an interplay between redox partner affinity and substrate affinity for P450s (*79*). The binding affinity of BNZ to

CYP2B4 may be enhanced by the interaction between CYP2B4 and CPR and vice-versa. Thus, we hypothesized that an alteration in CYP2B4 – CPR complex formation by CYP2E1 should be reflected in modifications in the kinetic parameters of CYP2B4 for BNZ, its substrate. Titrating increasing concentrations of BNZ with fixed concentrations of CYP2B4 and equal concentrations of CPR were used to determine the K_M and k_{cat} of CYP2B4 for its substrate. The experiment was repeated with a four-fold concentration of CYP2E1 over CYP2B4. The results of the experiment showed that the K_M increases by 8-fold, yet the k_{cat} remains almost unchanged. These results are illustrated in Figure 8 and Table 2. If the increase in K_M for BNZ is due to competition between CYP2E1 and CYP2B4 to be reduced by CPR, then supplying saturating concentrations of CPR should alter the binding equilibrium in favor of the CYP2B4 – CPR complex. This is demonstrated by the recovery of CYP2B4 activity at high concentrations of CPR, which is seen in Figure 8. Thus, the K_M and k_{cat} of CYP2B4 for BNZ in the absence and presence of CYP2E1 was determined under saturating concentrations of CPR, where CPR was 5-fold over the concentration CYP2B4. The results indicated that the presence of saturating concentrations of CPR enhanced the K_M of CYP2B4 for BNZ. In the absence of CYP2E1, there was a 28% enhancement. While in the presence of CYP2E1, there was a 75% enhancement relative to the sub-saturating concentration of CPR. These results are consistent with the data shown in Figure 8. Together these results suggest that the presence of saturating CPR reduces the inhibitory effects of CYP2E1 on CYP2B4. The removal of this inhibition caused by CYP2E1 leads to an incomplete yet significant recovery of the K_M of CYP2B4 for BNZ.

Table 2

	CYP2B4			
	Control	**Plus CYP2E1**	**Plus saturating CPR**	**Plus CYP2E1 and saturating CPR**
K_M (mM)	0.075 ± 0.010	0.60 ± 0.13	0.17 ± 0.051	0.060 ± 0.012
k_{cat} (min^{-1})	32 ± 0.78	33 ± 3.7	30 ± 3.0	35 ± 1.6

Table 2. The effect of CYP2E1 WT and CPR on K_M and k_{cat} values for the metabolism of BNZ by CYP2B4. Measuring formaldehyde formation using Nash reagent was used to determine the rate of BNZ N-demethylation by CYP2B4 as described in Materials and Methods. These measurements are demonstrated in Figure 8.

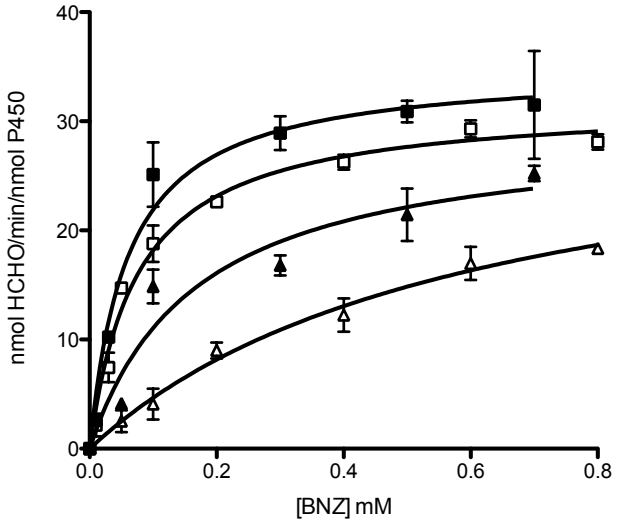

Figure 8. Effect of CYP2E1 and CPR on the kinetics of BNZ metabolism by CYP2B4. To investigate the effect that CYP2E1 has on CYP2B4 substrate affinity, the K_M and the k_{cat} values for BNZ metabolism by CYP2B4 were determined. The experiments had 0.50 μM CYP2B4, which was then titrated with increasing concentrations of BNZ as described in Materials and Methods. The method was conducted under the following conditions, (□) 0.50 μM CPR, (△) 0.50 μM CPR + 2 μM CYP2E1, (▲) 2.50 μM CPR + 2 μM CYP2E1, and (■) 2.50 μM CPR.

The effect of CYP2E1 on the Spectral Binding Constant (K_s) of BNZ CYP2B4. The incubation of CYP2B4 with excess CPR was preformed in attempt to decrease the K_M of BNZ for CYP2B4 to that observed in the absence of 2E1, but this was only partially successful, as shown in Table 2 and Figure 8. From this information, we hypothesized that an additional mechanism of substrate inhibition may be responsible for the observed difference. Previous CYP2B4 inhibition studies by CYP2E1 were performed in the presence of excess BNZ (1.2 mM). Thus a disturbance in CYP2B4's affinity for BNZ by the presence of CYPR2E1 may have been overlooked in these past studies. It is known that BNZ induces a type I spectral shift of CYP2B4, but BNZ does not cause this shift in CYP2E1 (data not shown). The type I spectral shift of CYP2B4 can be used to determine the effect of CYP2E1 on CYP2B4's affinity for its substrate, BNZ. The data in Figure 9A, C show that BNZ binds to CYP2B4 with a K_s of 11.4 μM, and that in the presence of CYP2E1, (Figure 9B, C) the K_s increases by 30 fold to 339 μM. These results show that CYP2E1 not only inhibits the affinity of CYP2B4 for CPR, but that CYP2E1 also inhibits CYP2B4's affinity for BNZ.

Figure 9A

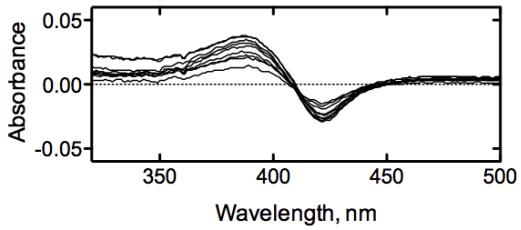

Figure 9B

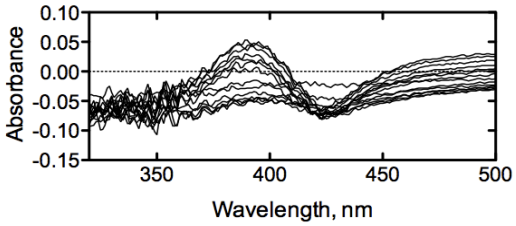

Figure 9C

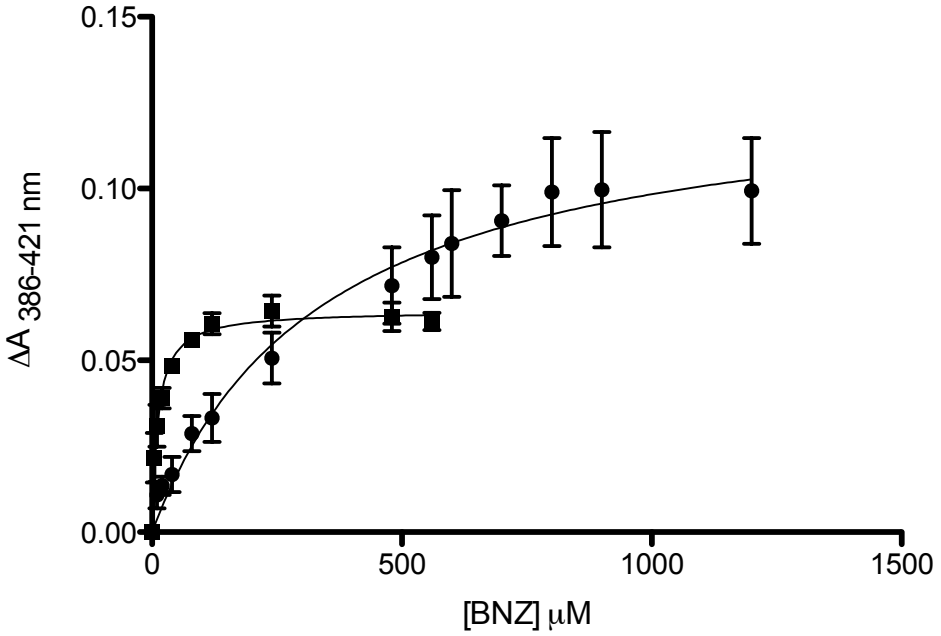

Figure 9. Type I spectral binding titrations for the binding of BNZ to CYP2B4. The spectral changes at 386 nm and at 421 nm were induced by the addition of increasing concentrations of BNZ to 1 μM CYP2B4, as shown in **Figure 9A** in the absence of CYP2E1. **Figure 9B** shows the spectral changes observed in the presence of 4 μM CYP2E1. The titrations were done as described in Materials and Methods. **Figure 9C** shows the absorbance changes plotted as a function of the BNZ concentration. The plot is used to determine K_s in the absence (■) and presence of CYP2E1 (●). The K_s values were calculated to be 11.4 μM ± 1.10 in the absence of CYP2E1 and to be 339 μM ± 60.2 in the presence of CYP2E1.

K_M and k_{cat} Values for the Interaction of CYP2E1 WT with CPR. To further investigate the kinetic basis for the inhibitory characteristics observed for CYP2E1, we determined the K_M of CYP2E1 for CPR using p-NP as the substrate. The ability of CYP2E1 to inhibit the formation of the CYP2B4 – CPR complex could be attributed to a higher affinity (lower K_M) of CYP2E1 for CPR compared to CYP2B4. However, our results showed that CYP2E1 and CYP2B4 have essentially the same affinity for CPR. CYP2E1 has a K_M of 0.02 μM, while CYP2B4 have a K_M of 0.15μM, as seen in Table 3. Interestingly, when the K_M of CYP2E1 for CPR was measured in the presence of CYP2B4, a 65% decrease in the K_M was observed, as shown in Figure 10 and Table 3. The final K_M value of 0.08 μM is close to the K_i value of CYP2E1 for the CYP2B4 – CPR complex of 0.05 μM. This suggests that the presence of CYP2B4 enhances the formation of the CYP2E1 – CPR complex.

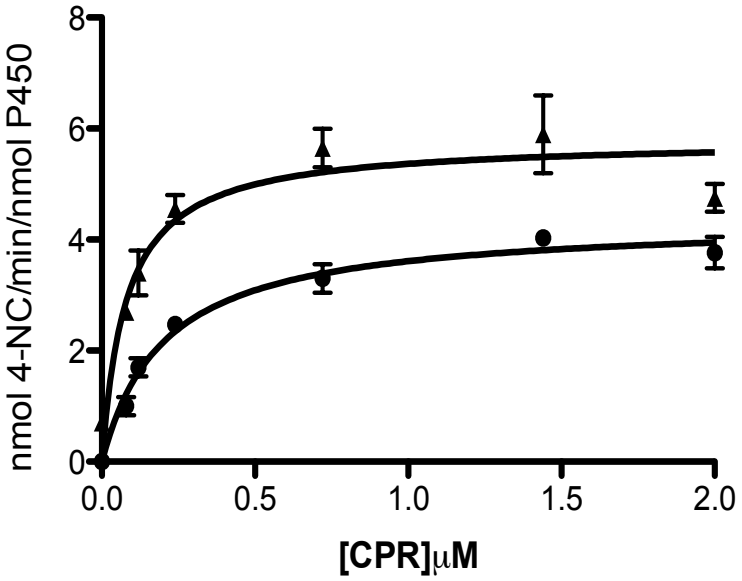

Figure 10. The effect of CYP2B4 on the K_M and k_{cat} of CYP2E1 for CPR. Using a fixed concentration of CYP2E1 (0.1 μM) and increasing concentration of CPR, the hydroxylation of p-NP was measured in the absence (●) or presence of 0.1 μM CYP2B4 (▲) as described in Materials and Methods. The error bars are the standard deviations from three measurements.

Table 3

	CYP2E1 WT	
	Control	**Plus CYP2B4**
K_M (μM)	0.21 ± 0.030	0.080 ± 0.022
k_{cat} (min^{-1})	4.4 ± 0.020	5.8 ± 0.033

Table 3. The K_M and k_{cat} of CYP2E1 WT for CPR in the absence and presence of CYP2B4. Reconstitution mixtures were made of 0.1 μM of CYP2E1 with varying concentrations of CPR in the presence and absence of 0.1 μM of CYP2B4. The reconstituted mixtures were added to 50 mM of potassium phosphate buffer (pH 7.4), 0.3 mM pNP, and 2 mM ascorbic acid after reconstitution. The reactions were initiated by

adding 0.4 mM NADPH and allowed to proceed for 20 min at 37^{o}C and then they were quenched with TCA. Measuring absorbance at 510 nm was used to determine the amount of 4-NC formed after the addition of NaOH.

Discussion:

Despite having known for almost forty years that P450s exist in vast excess over CPR in the endoplasmic reticulum, very little is know about the spatial distribution of P450s in the membrane (*34, 35*). There is even a greater mystery about how the difference in the molar ratios of P450 to CPR impacts the pharmacokinetic profile of drugs that mainly undergo P450-mediated phase I drug metabolism. The reductase forms a 1:1 complex with P450. Due to the disparity in the molar ratios of P450 and CPR it is highly improbable that, at any given time, every P450 will be interacting with a molecule of CPR. From this, it can be inferred that a significant percentage of the total microsomal P450 will be spatially incapable of receiving electrons from the CPR, thus these P450s are rendered metabolically silent. Cytochrome b_5 (cyt b_5) is known to participate in the reduction of P450s and therefore may ease the strain imposed by limited CPR concentrations. Cyt b_5 has been postulated to only donate the second electron in the P450 catalytic cycle; however, these results have been highly isoform and substrate-dependent. Despite the overall tertiary structure of mammalian P450s being highly conserved, the amino acid composition of the regions proposed to interact with CPR is highly variable. Thus, there is a possibility that significantly less than stoichiometric amounts of hepatic CPR relative to P450, along with variation in the nature of the interactions between different P450s and CPR may lead to favorable status for some P450s in the competition for CPR. This will have a significant impact on the reduction of the P450 heme and bound oxygen, ultimately leading to xenobiotic metabolism.

Often P450s have overlapping specificities. For a successful study to examine the

catalytic consequences of P450 – P450 interactions in a mixed reconstituted system, specific substrates for each P450 must be used. In this study, specific substrates were identified for CYP2E1 and CYP2B4. It is known that CYP2B4 metabolizes BNZ with high catalytic activity. Moreover, BNZ is not metabolized by CYP2E1, even at high concentrations of protein and substrate (data not shown). Additionally, BNZ does not induce a spectral change in CYP2E1's heme, indicating that CYP2E1 does not bind BNZ (data not shown), thus BNZ is an excellent substrate to assess CYP2B4 metabolism in a reconstituted system containing CYP2E1. CYP2E1 hydroxylates p-NP to produce 4-NC. By measuring the absorbance at 512 nm, 4-NC can be detected spectrophotometrically. Furthermore, p-NP is not metabolized by CYP2B4, and CYP2B4 does not bind p-NP. Thus BNZ was used as a probe substrate for CYP2B4 activity, while p-NP was used as the probe substrate for CYP2E1 activity. The rate of the first electron transfer, from CPR to CYP2E1 and CYP2B4 was also measured in the absence and presence of substrate. The results of this experiment showed that BNZ enhances the rate of electron transfer for CYP2B4, but BNZ does not enhance the rate for CYP2E1 (data not shown). On the other hand, p-NP had no effect on the reduction CYP2B4 or CYP2E1 (data not shown). From these results, we can exclude the possibility that the inhibitory properties of CYP2E1 towards CYP2B4 are caused by an enhanced transfer process induced by BNZ binding to CYP2E1.

By reacting P450s with peroxides such as tert-butyl hydroperoxide (tBHP), P450s are capable of generating the ferrous hydro-peroxy intermediate. The ferrous hydro-peroxy intermediate is the precursor to compound I in the catalytic cycle. The ability of P450s to

form the ferrous hydro-peroxy intermediate from reacting with peroxides allows P450s to bypass the need of CPR to deliver two electrons and the activated oxygen in the catalytic cycle. This property makes t-BHP a useful experimental tool to examine the catalytic integrity of the heme in the absence of CPR. CYP2B4 activity supported by CPR and tBHP were measured to be able to distinguish P450-P450 interactions from P450-CPR interactions that maybe responsible for the observed inhibition. Additionally, the studies were done in the presence of excess substrate (1.2 mM BNZ). The excess substrate allows differentiation between the effects of CYP2E1 on CYP2B4's affinity for CPR from CYP2E1's effect on CYP2B4's affinity for its substrate, BNZ. The results of the experiment showed that CYP2B4 was resistant to inhibition by CYP2E1 in the presence of tBHP. While CYP2B4 lost up to 80% of its BNZ activity in the presence of CPR, these results suggest that CPR is implicated in the inhibitory phenomenon observed in Figure 3A. We investigated whether the CYP2E1 variant (Y422D) could alter the extent of inhibition of CYP2B4 to further analyze the contribution of CYP2E1 – CPR interactions to the inhibition of CYP2B4. The CYP2E1 variant (Y422D) has a mutation in the proximal site that reduces its apparent binding to CPR by approximately 50%, as shown in Figure 4. The results showed that the extent of CYP2B4 inhibition by the CYP2E1 variant is significantly less than WT CYP2E1. These results also support the suggestion that CYP2E1 – CPR interactions have a role in the loss of CYP2B4 activity supported by CPR.

Furthermore, the data acquired for the K_M of CYP2B4 for CPR supports the idea that CYP2E1 interferes with CYP2B4 – CPR complex formation. The CYP2B4 K_M value for

CPR demonstrated that low concentrations of CYP2E1 elevated the K_M for CPR by up to13-fold with a negligible effect on k_{cat} relative to samples that did not include CYP2E1. At higher concentrations of CYP2E1, there is decease in the K_M of CYP2B4 for CPR but there is a concomitant reduction in the k_{cat} by 13-fold. Inverse plots of velocity as a function of CPR concentration exposes that CYP2E1 behaves as both a competitive and noncompetitive inhibitor of the CYP2B4 – CPR interaction. We plotted $K_{M\ obs}$ as a function of CYP2E1 concentrations to approximate a kinetic constant for the observed competitive inhibition portion of CYP2E1 on CYP2B4. Then a linear regression analysis of this plot produced a straight line, which intersected with the *x*-axis at -0.05μM. This linear regression plot demonstrates that inhibition of CYP2B4 by CYP2E1 is very potent. Furthermore, a global non-linear analysis done by GraphPad prism of the same data revealed a similar K_i.

These results are intriguing to contemplate, especially in relation to the P450's individual K_M values for CPR. For two P450s that are competing for the same functional binding site of CPR, the specificity should be determined by the individual K_M values of the P450s for CPR. That is, the specificity will distinguish between binding of the two competing P450s for CPR. However, the K_M values measured for CYP2B4 and CYP2E1 for CPR are virtually identical. The K_M value of CYP2B4 for CPR was 0.16 μM while the K_M of CYP2E1 for CPR was 0.20 μM. Thus, it would be expected that both P450s could compete with each other equally for CPR. However, the data indicates that CYP2E1 is significantly more effective at competing with, whereas 2B4 did not compete with 2E1 for CPR as shown in Figure 3. This inconsistency in the competition between

CYP2B4 and CYP2E1 suggested that the competition between CYP2B4 and CYP2E1 for CPR did not proceed through a competitive binding of CPR. Backes and co-workers have suggested that the presence of one P450 may enhance the affinity of an other P450 for CPR (*41*). Determining the K_M and k_{cat} of CYP2E1 for CPR in the absence and presence of CYP2B4 showed that the k_{cat} increased by 1.4-fold to 5.8 min^{-1}, while the K_M decreased by 65% to 0.08μM. Remarkably, this value of the enhanced K_M is comparable to the K_i of CYP2E1 for the CYP2B4 – CPR complex. Hence, this data supports the idea that a decrease in the K_M of CYP2E1 for CPR in the presence of CPY2B4 may impact the inhibitory properties of CYP2E1.

One possible mechanism to explain the observed interactions would involve the conformational trapping of CPR by CYP2B4 and/or CYP2E1. The model for these interaction is illustrated in Figure 11. This model is based on a couple findings. The first finding is that the direct CYP2B4 – CYP2E1 interaction alone does not lead to inhibition of CYP2B4 activity in the presence of saturating concentrations of BNZ, as shown in Figure 3A. Secondly, this model is supported by the observation that CYP2B4 and CYP2E1 interact directly reduce the affinity of CYP2B4 for BNZ as shown in Figure 9. Additionally, the model is based on the observation that CYP2E1 has a higher K_M for CPR in the presence of CYP2B4 (Figure 10). It has been well established that macromolecular structures such as enzymes and RNA may experience conformational changes in solutions (*75, 80)*. These conformational changes are necessary for their catalytic activity (*81)*. The electron density of the hinge region connecting the FMN domain to the FAD domain in CPR is often disordered in the CPR crystal structures (*82*).

Recently completed mutagenesis studies have demonstrated that the hinge region plays a significant role in moving the two-flavin domains of CPR apart from each other. A disulphide bond, which is specifically engineered to hold the domains in place, limits this movement. With the disulphide bond in place, it was found that CPR exhibited a loss in activity (*83*). Since CPR posseses this highly flexible hinge region, a potential explanation for the enhancement of the K_M of CYP2E1 for CPR may be from a conformational trapping of CPR. CPR may be conformationally trapped by the binding of 2B4 at a non-functional site of CPR, trapping CPR in a specific conformation that makes it more favorable for CYP2E1 to bind at the proposed functional site, FMN. On the other hand, it is just as probable that CYP2E1 binds to CPR functional site and then traps CPR in a specific conformation. In this conformation, it may be more favorable for CYP2B4 to bind at the non-funcational site of CPR.

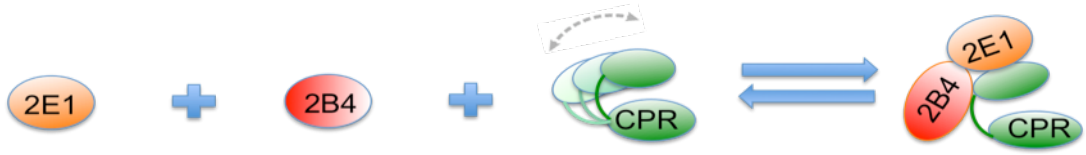

Figure 11. A tentative model for the CYP2B4-CYP2E1 synergistic interaction. Upon binding to a non-functional site on CPR, CYP2B4 traps CPR in a particular conformation that makes it more favorable for CYP2E1 to bind to the FMN domain or CYP2E1 binds at the functional site on CPR and traps CPR it in a particular conformation that makes it more favorable for CYP2B4 to bind at CPR's non-functional site. Both scenarios may give rise to an enhanced K_M of CYP2E1 for CPR.

In past studies that have examined the interactions between different P450s, the

inhibitory nature of CYP2E1 towards CYP2B4-mediated metabolism of BNZ and the enhancement of CYP2E1's K_M for CPR while using p-NP as the probe substrate has gone undetected. Studies by Kelly et. al. (*53*) have established that interactions between CYP1A2 and CYP2E1 result in a significantly enhanced rate of 7-ethoxyresorufin (7-ER) and 7-pentoxyresorufin (7-PR) metabolism. Nevertheless, when the interactions between CYP2E1 and CYP2B4 were investigated using 7-ER, 7-PR, and aniline as substrates, no functional interactions between CYP2E1 and CYP2B4 were observed. These results suggest that CYP2E1 and CYP2B4 do not form a P450 – P450 complex. Thus, the differences between the results of Kelly et al and our own are probably due to different isoforms of P450s used in the study, along with modification of the substrates used. As it has been previously shown, the interactions between P450s are dependent on the substrates under investigation (*34*).

Vatsis et. al. (*84*) demonstrated that by replacing the cysteine 436 with a serine in CYP2B4, that the mutant protein has the same K_M for reductase but is catalytically inactive. The CYP2B4 C436S mutant is unable to cleave the O-O bond in the catalytic cycle (*84)*. By use of this mutant, we attempted to examine the reduction step of CYP2B4 C463S in the presence of CYP2E1 to better understand the interactions between CYP2B4 and CYP2E1. This study would be the most direct way of studying interactions between CYP2E1, CYP2B4, and CPR. However, since both P450s absorb at the same wavelength (450 nm) when following reductions in the presence of CO, it was not possible to distinguish between the two isoforms during the reduction reaction. However, the CYP2B4 C463S absorbs at a different wavelength than CYP2E1, thus allowing the

isoforms to be distinguished. Unfortunately, in spite of our best attempts to express and purify the CYP2B4 C465S holoprotein, our attempts resulted in the production of significant amount apo-protein. Due to structural differences between the apo-protein and holo-protein, results from studies examining the competition for CPR would be skewed. Furthermore, the study involves titration of the mutant protein and due to the presence of the apo-protein, it would be difficult to quantify the amount of apo-protein, thus making the concentration of active P450 added unknown for the competition experiment.

To further understand the interactions occurring between CYP2B4, CYP2E1 and CPR there are a couple areas for future to studies. Sligar's lab has been examining P450s following incorporation into Nanodiscs, which are soluble nanoscale lipid bilayers (*85*). These Nanodiscs provide a model membrane system to study membrane proteins. They under go a simple self-assembly of a small lipid bilayer that is solubilized by a membrane scaffold protein along with the membrane protein of study. In Sligar's lab they have been able to successfully incorporate a single P450 and CPR into a Nanodisc. The Nanodisc technology would provide an alternative to studies in liposomes. By examining the interactions of CYP2B4, CYP2E1, and CPR in Nanodiscs the results of the studies will allow differentiation of the effects of oligomers on P450-P450 interactions. The results of these experiments will give greater insight to isoform interaction *in vivo*. Work on this project has begun; I started working on a procedure for the incorporation of CYP2E1 and CPR into Nanodiscs. The ultimate goal of this study would be to successfully

incorporate CYP2B4, CYP2E1, and CPR into a single Nanodisc to allow for further study.

Woodward et. al. have developed a method for the incorporation of heme analogs without exposing the protein to harsh denaturing conditions (*86*). This methodology allowed for the replacement of the heme iron with another transition metal in Nitric Oxide Synthase (NOS). NOS has been found to be very similar to P450. They both are heme-thiolate proteins, which have the same prosthetic group to perform similar oxidative reactions (*87*). In both P450 and NOS the electrons are supplied by a flavorprotein reductase, where the reductase is an integral part of the NOS (*87*). The structural and functional similarities between P450 and NOS make the methodology of Woodward et. al. promising for achieving iron replacement in P450s. The replacement of the heme iron with a transition metal would result in the P450 only weakly binding CO, and would result in silencing of one P450 at a time. With the ability to selectively silence an individual P450 isoform it would be possible to examine in greater detail interactions between P450 isoforms. For our studies the ability to selective silence a P450 would allow for greater opportunities to examine and understand the interactions between CYP2E1 and CYP2B4.

In the big pharmaceutical company setting a significant amount of effort is made to understand and predict *in vivo* pharmacokinetic profiles of drugs and compounds from *in vitro* data (*88*). Protein-protein interactions in the P450 system, such as the ones described here, may confound *in vitro – in* vivo drug metabolism extrapolations. Thus, it

is critical that in-depth kinetic studies are conducted to determine the kinetic basis and associated kinetic constants that govern these interactions. Obtaining information from studies such as these is invaluable, as this information will play an important role in improving our ability to predict, for example, drug clearance and drug-drug interactions from *in vitro* data.

The conclusions presented in this paper illustrate that human CYP2E1 is an inhibitor of CYP2B4 activity. This inhibition by CYP2E1 is mediated indirectly through competition for CPR, while also being through direct CYP2E1 – CYP2B4 interactions. It was necessary to distinguish between CYP2E1 inhibition of CYP2B4 activity that is mediated directly by the CYP2E1-CYP2B4 interactions from competition between these two P450s for CPR. In order to differentiate between these types of inhibition, we evaluated whether increasing concentrations of CYP2E1 could inhibit CYP2B4's activity supported by tBHP in the absence of CPR and with a saturating concentration of BNZ. The results of this experiment showed that the loss in CYP2B4 activity was minimal in comparison to CYP2B4's loss in activity in the presence of CPR. Thus, we were able to conclude that inhibition of CYP2B4 by CYP2E1 under saturating concentrations of substrate is probably mediated by competition for CPR. The results from determining CYP2B4's K_M for CPR under varying concentrations of CYP2E1 established that CPR was implicated in the inhibitory action of CYP2E1 and the measurements of CYP2E1's K_M for CPR were significantly enhanced by the presence of CYP2B4. Additionally, it was observed that CYP2E1 can perturb CYP2B4's affinity for BNZ as established by measurement of

BNZ's substrate dissociation constant for CYP2B4 in the absence and presence of CYP2E1.

References:

1. Klingenberg, M. (1958). Pigments of Rat Liver Microsomes. *Arch. Biochem. Biophys.* **75**, 376-386

2. Omura, T., and R. Sato (1964). The Carbon Monoxide-binding Pigment of Liver Microsomes. *J. Biol. Chem.* **239**, 2379-2385

3. Conney, A. H., E.C. Miller, and A.J. Miller (1956). The Metabolism of Methylated Aminoazo Dyes V. Evidence for Induction of Enzyme Synthesis in the Rat by 3-Methylcholanthrene. *Cancer Res.* **16**, 450-459

4. Brodie, B. B., J.R. Gillette, and B.N. LaDu (1958). Enzymatic Metabolism of Drugs and Other Foreign Compounds. *Annu. Rev. Biochem.* **27**, 427-454

5. Kamataki, T., and R.A. Neal (1976). Metabolism of Diethyl *p*-Nitrophenyl Phosphorothionate (parathion) by a Reconstituted Mixed-Function Oxidase Enzyme Stystem: Studies of the Covalent Binding of the Sulfur Atom. *Mol. Pharmacol.* **12**, 933-944

6. Capdevila, J. H., V.R. Holla, and J.R. Falck (2005) *Cytochrome P450: Structure, Mechanism, and Biochemistry (3nd Ed.) Ortiz de Montellano, P. R. Ed. Plenum Press, New York*, 531-551

7. Estabrook, R. W., D.Y. Cooper, and O. Rosenthal (1963). The light Reversible Carbon Monoxide Inhibition of the Steroid C21-Hydroxylase System of the Adrenal Cortex. *Biochem. Z.* **338**, 741-755

8. Cooper, D.Y., S.S. Levin, S. Narasimhulu, O. Rosenthal, and R.W. Estabrook (1965) Photochemical Action Spectrum of ther Terminal Oxidase of Mixed Function Oxidase Systems. *Science* **147**, 400-402

9. Lu A.Y.H. and MJ Coon (1968) Role of hemoprotein P-450 in fatty acid omega-hydroxylation in a soluble enzyme system from liver microsomes. *J. Biol. Chem.* **243**, 1331–1332.

10. Lu A.Y.H., K.W. Junk , and M.J. Coon (1969) Resolution of the cytochrome P-450-containing omega-hydroxylation system of liver microsomes into three components. *J Biol Chem* **244**, 3714–3721.

11. Kaschnitz, R.M., and M.J. Coon (1975) Drug and Fatty Acid Hydroxylation by Solubilized Human Liver Microsomal Cytochrome P450-Phospholipid Requirement. *Biochem. Pharmacol.* **24,** 295-297

12. Wang, P., P.S. Beaune, and F.P. Guengerich (1980) Purification of Human Liver Cytochrome P450 and Comparison to the Enzyme Isolated from Rat Liver. *Arch. Biochem. Biophys.* **199**, 206-219

13. Imai, Y. and R. Sato (1966) Evidence for two forms of P-450 hemoprotein in microsomal membranes. *Biochem Biophys Res Commun* **23**, 5–11.

14. Sladek N.E. and G.J. Mannering (1966) Evidence for a new P-450 hemoprotein in hepatic microsomes from methylcholanthrene treated rats. *Biochem Biophys Res Commun* **22**, 668–674.

15. Gonzalez, F. J. (1989) The Molecular Biology of Cytochrome P450s *Pharmacol. Rev*. **40**, 243-288

16. Nebert, D. W., M. Adesnik, M.J. Coon, R.W. Estabrook, F.J. Gonzalez, and F.P. Guengerich (1987) The P450 gene superfamily: Recommended Nomenclature *DNA* **6**,1-11

17. Ravichandran, K. G., S.S. Boddupalli, C.A. Hasermann, J.A.Peterson, and J. Deisenhofer (1993) Crystal Structure of Hemoprotein Domain of P450BM-3, a Prototype for Microsomal P450's *Science* **261**, 731-736

18. Rowland, P., F.E. Blaney, M.G. Smyth, J.J. Jones, V. R. Leydon, A.K. Oxbrow, C. J. Lewis, M. G. Tennant, S. Modi, D.S. Eggleston, R.J. Chenery, and A.M. Bridges (2006) Crystal Structure of Human Cytochrome P450 2D5 *J. Biol. Chem.* **281**, 7614-7622

19. Williams, P. A., J. Cosme, D.M. Vinkovic, A. Ward, H.C. Angove, P.J. Day, C. Vonrhein, I.J. Tickle, and H. Jhoti (2004) Crystal Structure of Human Cytochrome P450 3A4 Bound to Metyrapone and Progesterone, *Science* **305**, 683-686

20. Meunier, B., S. P. de Visser, and S. Shaik (2004) Mechanism of Oxidation Reactions Catalyzed by Cytochrome P450 Enzymes. *Chem. Rev.* **104**, 3947-3980

21. Correia, M. A., and Ortiz de Montellano, P. R. (2005) *Cytochrome P450: Structure, Mechanism, and Biochemistry (3rd Ed.) Ortiz de Montellano, P. R. Ed. Kluwer Academic Plenum Publishers, New York*, 247-322

22. Guengerich, F.P. (2005) *Cytochrome P450: Structure, Mechanism, and Biochemistry (3rd Ed.) Ortiz de Montellano, P. R. Ed. Kluwer Academic Plenum Publishers, New York*, 377-463

23. Thomas, P. L., and E.F. Johnson (2005) *Cytochrome P450: Structure, Mechanism, and Biochemistry (3rd Ed.) Ortiz de Montellano, P. R. Ed. Kluwer Academic Plenum Publishers, New York*, 87-114

24. Scott, E. E., M. A. White, Y. A. He, E. F. Johnson, C. D. Stout, and J. R. Halpert (2004) Structure of Memmalian Cytochrome P450 2B4 complexed with 4-(4-Chlorophenyl_imidazole at 1.9-A Resolution, *J. Biol. Chem.* **279** 27294-27301.

25. Bernhardt, R. (2006) Cytochromes P450 as Versatile Biocatalysts. *J. of Biotech.* **124**, 128-145

26. Nelson, D. R., L. Koymans, and T. Kamataki (1996). P450 superfamily: Update on new sequence, gene mapping, accession numbers and nomenclature. *Pharmacogenetics* **6**, 1-42

27. Porter, T. D., and Coon, M. J. (1991) Cytochrome P-450. Multiplicity of isoforms, substrates, and catalytic and regulatory mechanisms, *J Biol Chem* **266**, 13469-13472.

28. Evans, W. E., and M. V. Relling (1999) Pharmacogenomics: translating functional genomics into rational therapeutics, *Science* **286**, 487-491.

29. Schenkman, J. B., H. Remmer, and R.W. Estabrook (1967) Spectral Studies of Drug Interaction with Hepatic Microsomal Cytochrome *Mol. Pharmacol.* **3**, 113-123

30. Groves, J.T. (2005) *Cytochrome P450: Structure, Mechanism, and Biochemistry (3rd Ed.) Ortiz de Montellano, P. R. Ed. Kluwer Academic Plenum Publishers, New York*, 1-34

31. Denisov, I. G., T. M. Makris, S. G. Sligar, and I. Schlichting (2005) Structure and chemistry of cytochrome P450, *Chem Rev* **105**, 2253-2277.

32. Rittle, J., and M. T. Green (2010) Cytochrome P450 compound I: capture, characterization, and C-H bond activation kinetics, *Science* **330**, 933-937.

33. N. N. Bumpus (2008) The effects of a naturally occurring genetic polymorphism on the catalytic properties of human cytochrome P450 2B6. *Thesis*

34. Cawley, G. F., C. J. Batie, and W. L. Backes (1995) Substrate-dependent competition of different P450 isozymes for limiting NADPH-cytochrome P450 reductase, *Biochemistry* **34**, 1244-1247.

35. Backes, W. L., and R. W. Kelley (2003) Organization of multiple cytochrome P450s with NADPH-cytochrome P450 reductase in membranes, *Pharmacol Ther* **98**, 221-233.

36. Estabrook, R.W., M.R. Franklin, B. Cohen, A. Shigamatzu, and A.G. Hildebrandt (1971). Biochemical and Genetic Factors Influencing Drug Metabolism: Influence of Hepatic Microsomal Mixed Function Oxidation Reactions on Cellular Metabolic Control. *Metabolism*. **20**, 187-199

37. Stier, A., and E. Sackmann (1973). Heterogeneous Lipid Distribution in Liver Microsomal Membranes. *Biochim. Ciophys. Acta* **311**, 400-408

38. Peterson, J. A., R. E. Ebel, D. H. O'Keeffe, T. Matsubara, and R. W. Estabrook (1976) Temperature dependence of cytochrome P-450 reduction. A model for NADPH-cytochrome P-450 reductase:cytochrome P-450 interaction, *J Biol Chem* **251**, 4010-4016.

39. Brignac-Huber, L., J. R. Reed, and W. L. Backes (2011) Organization of NADPH-cytochrome P450 reductase and CYP1A2 in the endoplasmic reticulum--microdomain localization affects monooxygenase function, *Mol Pharmacol* **79**, 549-557.

40. Eyer, C. S., and W. L. Backes (1992) Relationship between the rate of reductase-cytochrome P450 complex formation and the rate of first electron transfer, *Arch Biochem Biophys* **293**, 231-240.

41. Reed, J.R., W.L. Backes (2011) Formation of P450-P450 Complexes and Their Effect on P450 Function, *Pharmacol. Ther.* **133**, 299-310

42. Schreiber, G., G. Haran, and H.-X. Zhou (2009)Fundamental Aspects of Protein-Protein Association Kinetics, *Chem Review* **109**, 839-860.

43. Schreiber, G. (2002) Kinetic Studies of Protein-Protein Interactions, *Curr. Opin. Struct. Biol.* **12**, 41-47

44. West, S.B. and A.Y.H. Lu (1972) Reconstituted Liver Microsomal Enzyme System That Hydroxylates Drugs, Other Foreign Compounds and Endogenous Substrates. V. Competition between cytochrome P-450 and P-448 for reductase in 3,4-Benzpyrene Hydroxylation, *Arch Biochem Biophys* **153**, 298-303

45. Tan, Y., C.J. Patten, T. Smith, and C.S. Yang (1997) Competitive Interactions between Cytochromes P450 2A6 for NADPH-Cytochrome P450 Oxidoreductase in the Microsomal Membrane Produced by a Baculovirus Expression System. *Arch Biochem Biophys* **342**, 82-91

46. Cawley, G. F., S. Zhang, R. W. Kelley, and W. L. Backes (2001) Evidence supporting the interaction of CYP2B4 and CYP1A2 in microsomal preparations, *Drug Metab Dispos* **29**, 1529-1534.

47. Backes, W. L., C.J. Batie, and G.F. Cawley (1998) Interactions among P450 enzymes when combined in reconstituted systems: formation of a 2B4-1A2

complex with a high affinity for NADPH-cytochrome P450 reductase, *Biochemistry* **37**, 12852-12859.

48. Yamazaki, H., E. M. Gillam, M. S. Dong, W. W. Johnson, F. P. Guengerich, and T. Shimada (1997) Reconstitution of recombinant cytochrome P450 2C10(2C9) and comparison with cytochrome P450 3A4 and other forms: effects of cytochrome P450-P450 and cytochrome P450-b5 interactions, *Arch Biochem Biophys* **342**, 329-337.

49. Subramanian, M., M. Low, C. W. Locuson, and T. S. Tracy (2009) CYP2D6-CYP2C9 protein-protein interactions and isoform-selective effects on substrate binding and catalysis, *Drug Metab Dispos* **37**, 1682-1689.

50. Hazai, E., and D. Kupfer (2005) Interactions between CYP2C9 and CYP2C19 in reconstituted binary systems influence their catalytic activity: possible rationale for the inability of CYP2C19 to catalyze methoxychlor demethylation in human liver microsomes, *Drug Metab Dispos* **33**, 157-164.

51. Hu, Y., K. Krausz, H. V. Gelboin, and D. Kupfer (2004) CYP2C subfamily, primarily CYP2C9, catalyses the enantioselective demethylation of the endocrine disruptor pesticide methoxychlor in human liver microsomes: use of inhibitory monoclonal antibodies in P450 identification, *Xenobiotica* **34**, 117-132.

52. Alston, K., R.C. Robinson, S.S. Park, H.V. Gelboin, and F.K. Friedman (1990) Interaction Among Cytochrome P-450 in the Endoplasmic Reticulum: Detection of Chemically Cross-Linked Complexes with Monoclonal Antibodies, *J. Biol Chem.* **266**, 735-739

53. Kelley, R. W., D. Cheng, and W. L. Backes (2006) Heteromeric complex formation between CYP2E1 and CYP1A2: evidence for the involvement of electrostatic interactions, *Biochemistry* **45**, 15807-15816.

54. Subramanian, M., H. Tam, H. Zheng, and T. S. Tracy (2010) CYP2C9-CYP3A4 protein-protein interactions: role of the hydrophobic N terminus, *Drug Metab Dispos* **38**, 1003-1009

55. Orme-Johnson, W.H. and D.M. Ziegler (1965). Alcohol mixed function oxidase activity of mammalian liver micoromes. *Biochm. Biophys. Res. Commun.* **21**, 78-82

56. Porubsky, P. R., K. M. Meneely, and E. E. Scott (2008) Structures of human cytochrome P-450 2E1. Insights into the binding of inhibitors and both small molecular weight and fatty acid substrates, *J Biol Chem* **283**, 33698-33707.

57. Patten, C. J., P. E. Thomas, R. L. Guy, M. Lee, F. J. Gonzalez, F. P. Guengerich, and C. S. Yang (1993) Cytochrome P450 enzymes involved in acetaminophen activation by rat and human liver microsomes and their kinetics, *Chem Res Toxicol* **6,** 511-518.

58. Levin, W., P. E. Thomas, N. Oldfield, and D. E. Ryan (1986) N-demethylation of N-nitrosodimethylamine catalyzed by purified rat hepatic microsomal cytochrome P-450: isozyme specificity and role of cytochrome b5, *Arch Biochem Biophys* **248**, 158-165.

59. Guengerich, F. P., D. H. Kim, and M. Iwasaki (1991) Role of human cytochrome P-450 IIE1 in the oxidation of many low molecular weight cancer suspects, *Chem Res Toxicol* **4**, 168-179.

60. Oneta, C. M., C.S. Lieber, J. Li, S. Ruttimann, B. Schmid, J. Lattmann, A. S. Rosman, and H. K. Seitz (2002) Dynamics of cytochrome P4502E1 activity in man: induction by ethanol and disappearance during withdrawal phase, *J Hepatol* **36**, 47-52.

61. Johansson, I., G. Ekstrom, B. Scholte, D. Puzycki, H. Jornvall, and M. Ingelman-Sundberg. (1988) Ethanol-, fasting-, and acetone-inducible cytochromes P-450 in rat liver: regulation and characteristics of enzymes belonging to the IIB and IIE gene subfamilies, *Biochemistry* **27**, 1925-1934.

62. Dey, A., and A. I. Cederbaum (2006) Alcohol and oxidative liver injury, *Hepatology* **43**, S63-74.

63. Walsky, R. L., A. V. Astuccio, and R. S. Obach (2006) Evaluation of 227 drugs for in vitro inhibition of cytochrome P450 2B6, *J Clin Pharmacol* **46**, 1426-1438.

64. Wang, H., and L. M. Tompkins (2008) CYP2B6: new insights into a historically overlooked cytochrome P450 isozyme, *Curr Drug Metab* **9**, 598-610.

65. Scott, E. E., M. Spatzenegger, and J. R. Halpert (2001) A truncation of 2B subfamily cytochromes P450 yields increased expression levels, increased solubility, and decreased aggregation while retaining function, *Arch Biochem Biophys* **395**, 57-68.

66. Oezguen, N., S. Kumar, A. Hindupur, W. Braun, B. K. Muralidhara, and J. R. Halpert (2008) Identification and analysis of conserved sequence motifs in cytochrome P450 family 2. Functional and structural role of a motif 187RFDYKD192 in CYP2B enzymes, *J Biol Chem* **283**, 21808-21816.

67. Gay, S. C., M. B. Shah, J. C. Talakad, K. Maekawa, A. G. Roberts, P. R. Wilderman, L. Sun, J. Y. Yang, S.C. Huelga, W. X. Hong, Q. Zhang, C. D. Stout, and J. R. Halpert (2010) Crystal structure of a cytochrome P450 2B6 genetic variant in complex with the inhibitor 4-(4-chlorophenyl)imidazole at 2.0-A resolution, *Mol Pharmacol* **77**, 529-538.

68. Scott, E. E., Y. A. He, M. R. Wester, M. A. White, C. C. Chin, J. R. Halpert, E. F. Johnson, and C. D. Stout (2003) An open conformation of mammalian cytochrome P450 2B4 at 1.6-A resolution, *Proc Natl Acad Sci U S A* **100**, 13196-13201.

69. Pratt-Hyatt, M., H. L. Lin, and P. F. Hollenberg (2010) Mechanism-based inactivation of human CYP2E1 by diethyldithocarbamate, *Drug Metab Dispos* **38**, 2286-2292.

70. Zhang, H., S. C. Im, and L. Waskell (2007) Cytochrome b5 increases the rate of product formation by cytochrome P450 2B4 and competes with cytochrome P450 reductase for a binding site on cytochrome P450 2B4, *J Biol Chem* **282**, 29766-29776.

71. Vermilion, J. L., and M. J. Coon (1978) Purified liver microsomal NADPH-cytochrome P-450 reductase. Spectral characterization of oxidation-reduction states, *J Biol Chem* **253**, 2694-2704.

72. Nash, T. (1953) The colorimetric estimation of formaldehyde by means of the Hantzsch reaction, *Biochem J* **55**, 416-421.

73. Kenaan, C., H. Zhang, E. V. Shea, and P. F. Hollenberg (2011) Uncovering the role of hydrophobic residues in cytochrome P450-cytochrome P450 reductase interactions, *Biochemistry* **50**, 3957-3967.

74. Kakkar, T., H. Boxenbaum, and M. Mayersohn (1999) Estimation of Ki in a competitive enzyme-inhibition model: comparisons among three methods of data analysis, *Drug Metab Dispos* **27**, 756-762.

75. Zhang, H., C. Kenaan, D. Hamdane, D., G. H. Hoa, and P. F. Hollenberg (2009) Effect of conformational dynamics on substrate recognition and specificity as probed by the introduction of a de novo disulfide bond into cytochrome P450 2B1, *J Biol Chem* **284**, 25678-25686.

76. Lin, H. L., E. Myshkin, L. Waskell, and P. F. Hollenberg (2007) Peroxynitrite inactivation of human cytochrome P450s 2B6 and 2E1: heme modification and site-specific nitrotyrosine formation, *Chem Res Toxicol* **20**, 1612-1622.

77. Bridges, A., L. Gruenke, Y. T. Chang, I. A. Vakser, G. Loew, and L. Waskell (1998) Identification of the binding site on cytochrome P450 2B4 for cytochrome b5 and cytochrome P450 reductase, *J Biol Chem* **273**, 17036-17049.

78. Miwa, G. T., S. B. West, M. T. Huang, and A. Y. Lu (1979) Studies on the association of cytochrome P-450 and NADPH-cytochrome c reductase during catalysis in a reconstituted hydroxylating system, *J Biol Chem* **254**, 5695-5700.

79. Bonfils, C., C. Balny, and P. Maurel (1981) Direct evidence for electron transfer from ferrous cytochrome b5 to the oxyferrous intermediate of liver microsomal cytochrome P-450 LM2, *J Biol Chem* **256**, 9457-9465.

80. Zhang, Q., Stelzer, A. C., Fisher, C. K., and Al-Hashimi, H. M. (2007) Visualizing spatially correlated dynamics that directs RNA conformational transitions, *Nature 450*, 1263-1267.

81. Henzler-Wildman, K. A., Lei, M., Thai, V., Kerns, S. J., Karplus, M., and Kern, D. (2007) A hierarchy of timescales in protein dynamics is linked to enzyme catalysis, *Nature 450*, 913-916.

82. Hamdane, D., Xia, C., Im, S. C., Zhang, H., Kim, J. J., and Waskell, L. (2009) Structure and function of an NADPH-cytochrome P450 oxidoreductase in an open conformation capable of reducing cytochrome P450, *J Biol Chem 284*, 11374-11384.

83. Xia, C., Hamdane, D., Shen, A. L., Choi, V., Kasper, C. B., Pearl, N. M., Zhang, H., Im, S. C., Waskell, L., and Kim, J. J. (2011) Conformational changes of NADPH-cytochrome P450 oxidoreductase are essential for catalysis and cofactor binding, *J Biol Chem 286*, 16246-16260.

84. Vatsis, K. P., H.M. Peng, and M. J. Coon (2002) Replacement of active-site cysteine-436 by serine converts cytochrome P450 2B4 into an NADPH oxidase with negligible monooxygenase activity, *J. Inorgan. Biochem.* **91**, 542-553

85. Denisov, I. G. and S. G. Sligar (2010) Cytochrome P450 in Nanodisc., *Biochem et Bipphys Acta* **1814** 223-229

86. Woodward, J.J., N. I. Martin, and M. A. Marletta (2006) An *Escherichia coli* expression-based method for heme substitution. *Nature Meth.* **24** 43-45

87. Gorren, A.C. and B. Mayer (2007) Nitroc –oxide synthase: a cytochrome P450 family foster child, *Bioch Biochys Acta.* **1770** 432-445

88. Rostami-Hodjegan, A., and Tucker, G. T. (2007) Simulation and prediction of in vivo drug metabolism in human populations from in vitro data, *Nat Rev Drug Discov 6*, 140-148.

Acknowledgements:

I am deeply grateful to Dr. Paul Hollenberg for giving me the opportunity to conduct research in his laboratory over the past four years. His kindness, support, encouragement, and knowledge of science were critical in my research and have helped my development as a student and researcher. Thank you, Dr. Hollenberg!

I would like to give a special thanks to the doctoral candidate, Cesar Kenaan, who has been my mentor in the lab. He taught me about cytochrome P450 and how to be an independent scientist. He provided counsel on professional aspirations and he has been a good friend.

I would also like to thank Dr. Haoming Zhang, Hsia-Lien Lin, and Diane Calinski for their time that was spent training and helping with my project. Additionally, I would like to thank all the members of the Hollenberg lab: Chitra Sridar, Jaime D'Agostino, Vyvyca Walker, Hemali Amunugama, and Sarah Ney. They all helped further my interest in research. Outside of the lab, I would like to thank Dr. Ballou for his help and time spent training and allowing the use the stopped flow machine.

Furthermore, I would like to University of Michigan Pharmacology Department for their financial support through my research. I am thankful to the University of Vermont Pharmacology Department for my introduction to pharmacology research, especially Dr.

Mark T. Nelson for his continued guidance as a mentor in science and as a wonderful uncle. Thank you, Mark!

Finally, I would like to thank my family: my mother, father, and brother, Tim, for their support and continuing belief in my decisions and me. I thank my friends, especially James Brunner, for their interest in and patience during my scientific endeavors.